MISCELLANEOUS PAPER GL-82-13

MODELING OF ELECTROKINESIS

by

James B. Warriner, Perry A. Taylor

Geotechnical Laboratory
U. S. Army Engineer Waterways Experiment Station
P. O. Box 631, Vicksburg, Miss. 39180

September 1982

Final Report

Prepared for Assistant Secretary of the Army (R&D)
Department of the Army
Washington, D. C. 20315

Under ILIR Project No. 4A161101A91D, Task A2
Work Unit 141

REPORT DOCUMENTATION PAGE

READ INSTRUCTIONS BEFORE COMPLETING FORM

1. REPORT NUMBER: Miscellaneous Paper GL-82-13
2. GOVT ACCESSION NO.:
3. RECIPIENT'S CATALOG NUMBER:

4. TITLE (and Subtitle): MODELING OF ELECTROKINESIS
5. TYPE OF REPORT & PERIOD COVERED: Final report
6. PERFORMING ORG. REPORT NUMBER:

7. AUTHOR(s): James B. Warriner, Perry A. Taylor
8. CONTRACT OR GRANT NUMBER(s):

9. PERFORMING ORGANIZATION NAME AND ADDRESS: U. S. Army Engineer Waterways Experiment Station, Geotechnical Laboratory, P. O. Box 631, Vicksburg, Miss. 39180
10. PROGRAM ELEMENT, PROJECT, TASK AREA & WORK UNIT NUMBERS: Project 4A161101A91D, Work Unit 141

11. CONTROLLING OFFICE NAME AND ADDRESS: Assistant Secretary of the Army (R&D), Department of the Army, Washington, D. C. 20315
12. REPORT DATE: September 1982
13. NUMBER OF PAGES: 56

14. MONITORING AGENCY NAME & ADDRESS (if different from Controlling Office):
15. SECURITY CLASS. (of this report): Unclassified
15a. DECLASSIFICATION/DOWNGRADING SCHEDULE:

16. DISTRIBUTION STATEMENT (of this Report):

Approved for public release; distribution unlimited.

17. DISTRIBUTION STATEMENT (of the abstract entered in Block 20, if different from Report):

18. SUPPLEMENTARY NOTES

Available from National Technical Information Service, 5285 Port Royal Road, Springfield, Va. 22151

19. KEY WORDS (Continue on reverse side if necessary and identify by block number)

Electrokinetic effects
Geological investigations
Mathematical models
Water flow
Water properties

20. ABSTRACT (Continue on reverse side if necessary and identify by block number)

Electrokinetic streaming potentials were measured in typical geological materials using specially constructed apparatus to model water flow through subsurface flow paths.

The apparatus used for the study is described by this report as are the measurement techniques used. Comparisons between the observed electrokinesis phenomena and theoretical predictions are made.

(Continued)

20. ABSTRACT (Continued).

Conclusions resulting from this study include:

a. Studies of streaming potentials in typical geological materials should be concentrated in real geological environments.

b. Fluid electrical resistivity as influenced by dissolved ion content is more critical to streaming potential measurements than temperature influences and should be measured directly.

c. Contrary to the results of past studies of streaming potentials, it was found that metallic electrodes performed more satisfactorily than did nonpolarizable porous pot electrodes.

d. A relationship was observed between the flow rate of the water through the porous media and the electrical surface potential of the solid portion of the media. This relationship may provide a useful application of streaming potential surveys after further development.

e. The presence of appreciable amounts of clay in or near the water flow path through porous media degrades electrokinetic potential magnitudes and hinders streaming potential measurements.

PREFACE

The study reported herein was performed under the In-house Laboratory Independent Research (ILIR) Program, Project Number 4A161101A91D, Task Area 02, Work Unit Number 141, entitled "Field Modeling of Electrokinesis." Mr. F. R. Brown was the WES Technical Monitor.

The investigation was conducted by the U. S. Army Engineer Waterways Experiment Station (WES) during the period FY 80 - FY 82. The study was conducted under the direct supervision of Mr. J. S. Huie, Chief, Rock Mechanics Applications Group (RMAG), Geotechnical Laboratory (GL), and under the general supervision of Dr. D. C. Banks, Chief, Engineering Geology and Rock Mechanics Division (EGRMD), GL. Dr. W. F. Marcuson III was Chief, GL. Mr. J. B. Warriner, RMAG, prepared the report with the assistance of Mr. P. A. Taylor, RMAG. Mr. Taylor designed and constructed the experimental models and he and Mr. L. R. Flowers, RMAG, conducted all measurements.

Commanders and Directors of the WES during the investigation and preparation of this report were COL Nelson P. Conover, CE, and COL Tilford C. Creel, CE. Technical Director was Mr. Fred R. Brown.

CONTENTS

CONVERSION FACTORS, U. S. CUSTOMARY TO METRIC (SI)
UNITS OF MEASUREMENT

U. S. customary units of measurement used in this report can be converted to metric (SI) units as follows:

Multiply	By	To Obtain
feet	0.3048	metres
gallons (U. S. liquid)	3.785412	cubic decimetres
inches	2.54	centimetres
square feet	0.09290304	square metres

MODELING OF ELECTROKINESIS

PART I: INTRODUCTION

Background

1. The study reported herein consisted of a series of laboratory experiments intended to delineate major factors affecting the application of electrokinesis measurements to the location of water seepage paths. Electrokinesis is a term defined as relating to the motion of particles or liquids that results from or produces a difference of electric potential. The term electrokinesis has generally been applied to phenomena observed under laboratory conditions. When electrical potential surveys have been performed in the field for the purpose of describing the flow of subsurface water, the term "streaming potential" has been used to describe the same causative phenomenon as electrokinesis.

2. In 1979 an In-house Laboratory Independent Research project was proposed and approved. That proposal was made to assist in developing the U. S. Army Corps of Engineers (CE) capabilities to locate and describe subsurface paths of water seepage from reservoirs. The work was intended to result in field-usable geophysical survey techniques. The study had been in progress for several months before it was learned that an independent, separately sponsored effort was being carried on by personnel of the Earthquake Engineering and Geophysics Division (EEGD) that had been successful in emplacing a streaming potential measurement system at Gathright Dam, Virginia. The present study was reoriented at that time (1980) toward examining the factors affecting the magnitudes of measured streaming potentials.

Purpose

3. The purpose of this report is to describe a laboratory study of the phenomenon known variously as "streaming potential" or

"electrokinesis." The present study was performed under laboratory conditions on a large scale to simulate the occurrence of electrokinesis in typical geological materials. The intent of the study was to "bridge the gap" between an understanding of electrokinesis as it is observed in the laboratory and as it is observed in field surveys.

Scope

4. This report will present a background of electrokinesis as studied in the past. Brief descriptions will be given of the study methods proposed and used. The results obtained will be presented. The conclusions of the study will be presented.

PART II: LABORATORY STUDIES

General Review

5. Electrokinesis is defined as the electrical potential developed by the motion of some fluids flowing under pressure head over certain solid materials. The phenomenon is best observed when the flow is through narrow conduits within the solid material, e.g. the interconnected pore spaces of a porous granular medium. Electrokinesis was first observed by Helmholtz and reported by him in 1879 as it occurred when water was passed through a column of primarily quartz sand under pressure. Electrodes implanted within the sand developed an electrical potential which varied according to the pressure head applied to the flowing water. The expression describing the electrokinesis phenomenon as given by Smoluchowski (1951) is:

$$\frac{\Delta E_{sp}}{P} = D_{fl}\ \zeta_s / 4\pi\ \mu\ K_{fl} \qquad (1)$$

where

ΔE_{sp} = measured streaming potential (electrostatic volts)

P = applied pressure head (cm of water)

D_{fl} = dielectric constant of water (dimensionless)

ζ_s = surface potential of solid medium (electrostatic volts)

μ = viscosity of water (poise)

K_{fl} = specific conductance of water in flow channels (mho/cm)

6. The following is a qualitative description of the cause of streaming potential. Water possesses an electrically dipolar molecular structure in that the two hydrogen (positive charges) atoms are not diametrically opposed on the oxygen atom. They are, instead, at a relative angle of 111 deg to each other. Therefore, each molecule of water has a positively charged region (oriented between the positive hydrogen pair) and a diametrically opposed negatively charged region (oriented toward the negative oxygen atom). Many natural solid media possess a molecular structure in which the surface of the solid is characterized by negative

electric charges. Among these natural media with negative surface electric potentials are silica-based mineralogies and carbonates. Electrostatic attraction between the negatively charged grain surfaces and the positively charged pole of the water molecules causes a layer of water to affix itself to the grain surfaces leaving, in turn, a more weakly negatively charged region exterior to that first water layer. In non-flowing water-solid systems the thermal motion inherent to the individual water molecules prevents more than two layers to be electrostatically bound to the grain surfaces; hence the descriptive term "water double layer" is applied. If, however, the water phase of the system exhibits directional flow under a pressure gradient, then some molecules of the more weakly bound outer layer of molecules are swept away. The electrostatic charge imbalance that remains near the solid grain surfaces is negatively charged and is observed as an electric potential. That potential, represented herein as ΔE_{sp}, is the "streaming" or "electrokinetic" potential.

7. As described by Equation 1, the streaming potential is proportional to the pressure head applied to the water. The streaming potential is directly proportional to the dielectric constant of the water, D_{fl}. The dielectric constant of a polar liquid in an electric field is a measure of the force applied to components of that liquid by the field (Carson and Lorraine, 1962). The surface potential, ζ_s, or "zeta" potential represents the strength of the solid grain surface electric field. The viscosity of the water represented in Equation 1 partially governs the nature of flow through the pore spaces between the solid grains. The specific conductance to electricity of the fluid in the pore spaces (inverse of specific electrical resistivity, $K_{fl} = 1/\rho_{fl}$) governs the streaming potential by defining the intensity of electric potential difference from point to point that can remain in equilibrium (Carson and Lorraine, 1962).

8. Much of the laboratory study of streaming potential has been oriented toward explanation of the "self-potential" or "SP" logs performed routinely with the single-point electric logs in borehole geophysical surveys. The self-potential log is a passive measure of

electric potential measured continuously up boreholes relative to a surface grounding probe. Movement of water between a borehole and the surrounding geologic strata can arise because of (a) osmotic pressures tending to balance dissolved salt concentrations between the mud column and the formation fluids, or (b) because of hydrostatic pressure differentials between the mud column and the natural piezometric pressure, or (c) because of water movement across interfaces between different formations. Motion of the water, regardless of cause or orientation, develops an electrokinetic streaming potential which is the basis of the SP log. Bull and Gortner (1932) studied the effect of grain size on the electrokinetic potential. They found no linear relationship between pressure and the streaming potential when the quartz grains were of heterogeneous size mixture but did find a good relationship ($\Delta E_{sp} \propto \phi^{1/3}$, where ϕ is a grain diameter) for a homogeneously sized quartz aggregate. Wyllie (1951) examined drilling mud samples flowing through their own filtrates to separate the component of the cross-mud cake streaming potential from the self-potential log. Schriever and Bleil (1957) determined that the ratio $\Delta E_{sp}/P$ did not vary with the configuration of the quartz sand flow systems they studied, including the length of the columns of sand. Gondouin and Scala (1958) reexamined streaming potentials originating in the borehole mud cake and measured appreciable streaming potentials across shale samples in their laboratory. Bernstein and Scala (1959) studied streaming potentials at the interface separating two electrolytic solutions and also verified their existence and positive sign in shale samples.

9. A second area in the study of streaming potentials has been their relationship to the galvanic corrosion of metallic well screens. Mandal (1969) and Mandal and Edwards (1971) measured streaming potentials generated by water flowing through clean quartz sand between metallic screens. They measured the quartz zeta potential (using tap water), as -1250 mv and determined that screen incrustation could be initiated by the streaming potential. Theirs is the only experimental value for the natural grain surface potential.

10. A third area of past study of the streaming potential phenomenon has been its application to surface-based surveys to delineate subsurface paths of water seepage. Ogilvy, Ayed, and Bogoslovsky (1969) described a series of measurements in their laboratory and in two impounded reservoirs that used streaming potential values, water flow rate observations, and thermometry to locate paths of leakage from those reservoirs. Their laboratory studies were made using clean graded quartz sand in a glass flow tube through which various solutions of electrolytes were passed at controlled pressure heads. Their results from laboratory tests were as follows: with increase in permeability the ratio $\Delta E_{sp}/P$ increases to a maximum near $k = 60$–70 darcy (where k is the permeability to water) and then decreases to a constant value; $\Delta E_{sp}/P$ decreases with increasing electrolyte concentration (increasing electrical conductivity). They conclude that the process must occur under laminar flow conditions and "is apparently violated when the flow is turbulent, which takes place in rubble and big open fissures when the gradients are high." Ogilvy et al. (1969) caution, also, that the presence of clay in even part of the rock fissures will lead to positive values of streaming potentials as great as or greater than the negative potentials generated in clean fissures in rock. No differentiation was stated between streaming potential as it occurs in a silica-based geology as opposed to a carbonate geology. Ogilvy et al. (1969) dragged nonpolarizable potential electrodes along the reservoir bottoms to produce a series of traverse measurements of streaming potential. The electrodes were in the form of porous ceramic cylinders containing lead chloride coated electrodes immersed in potassium chloride solution. At one reservoir on "tuffaceous geology," leakage zones were identified by negative potential regions under the reservoir and the "amplitude of the anomaly indicates the intensity of leakage." However, distortions in the streaming potential measurements were seen to be caused by formation contacts, by clay concentrations in joints, and the presence and thickness of bottom mud. The interpreted investigations indicated -20 to -40 mv streaming potentials were correlated with four leakage zones through joints in basalt that flowed at 50 to 100 mm/sec. At the second

reservoir in quartzose conglomerate similar instrumentation was used and -10 to -30 mv streaming potential anomalies were correlated to leakage rates of 6-20 mm/sec. Positive electrical potential measurements in the latter survey were interpreted as the result of "lithologic peculiarities." Bogoslovsky and Ogilvy (1970) described a further application of streaming potential measurement to quantifying the rate of flow through leaky zones of reservoirs.

11. Applications of streaming potential surveys to seepage path location have been recognized by the Corps of Engineers since before 1972. A study at Walter F. George Reservoir in the South Atlantic Division was performed under contract using streaming potential measurements (Saucier 1970). Bates (1973) referred to streaming potential surveys as a possible search strategy for locating subsurface cavities. EM 1110-2-1802 (Department of the Army, Office, Chief of Engineers 1979) refers to streaming potential surveys as a potentially valuable geophysical method. Most recently the Earthquake Engineering and Geophysics Division (EEGD) of the WES has undertaken concept trial surveys at Gathright Dam, Virginia, and Clearwater Dam, Missouri (Cooper, Koester, and Franklin (1982) and Butler, Llopis, Koester, and Kean (1981)). The method of the surveys conducted by the EEGD has been to install semipermanent electrodes in traverses transecting geologically probable seepage paths which incorporate both intact and leaky zones. After obtaining a series of electrical potential measurements for comparison purposes from the individual electrodes comprising the transection, a series of perturbations were applied to the water flow regime in the form of increased pressure heads or electrical fluid conductivity changes or both.

Model Development

12. In modeling the flow of water through an aquifer a large rectangular box was first used. The box was made of wood and sat on level ground. Water seeped from the flow channel to the outside ground. Because of the many hydraulic and electrical flow paths to the ground, the

box was unsatisfactory as a model. A 3-1/16-in.* ID 2-ft-long plastic polyvinyl chloride (PVC) pipe was used to eliminate the different electrical flow paths to ground. Both of these models will be described as well as the technique used to run the tests on each model.

Box Flow Model

Box construction

13. A box was constructed of 3/4-in. waterproof plywood with inside dimensions of 12 ft long, 4 ft wide, and 4 ft high. Centered at the bottom on each end was a distribution plenum which was rigidly connected and sealed to the box. The two plenums were 4 in. long, 1 ft wide, and 1 ft high (length, width, and height are in the same directions as the large box dimensions). Each plenum contained the water port from the outside, and the 1-ft x 1-ft interior face plate of the plenum contained many holes allowing water to flow evenly into the sample. The modeled flow channels were 1 ft x 1 ft in cross section and extended the length of the box from plenum to plenum. See Figure 1 for details of the box construction.

Hydraulic system

14. The hydraulic system was designed to allow water to flow through one end of the box through the plenum and the 1-ft^2 cross section along the full length of the box into the other plenum and out of the box to an overflow with variable height capability. Manifolds and valves were used to reverse the direction of flow. Piezometers monitored the water pressure at different points in the system.

Water supply

15. The water supply was a 55-gal drum connected to a U. S. Army Engineer Waterways Experiment Station (WES) waterline. The drum sat on an elevated platform. At the bottom of the drum a manifold made of 1-in. pipe fittings was connected to allow water to be supplied to either plenum. A piezometer, made of 3/8-in. clear Tygon tubing, was

---

* A table of factors for converting U. S. customary units of measurement to metric (SI) units is presented on page 3.

placed vertically on the side of the barrel and a scale placed behind it and used for measuring water levels to ± 0.01 ft.

North-south inlets and outlets

16. The water leaving the manifold of the water supply flowed to either end of the box where valves allowed water to enter the box and plenum or go out of the overflow. If the water was to enter the manifold at one end, the overflow for that end was shut off. The water flowed through the first plenum, the sample, the second plenum, to the manifold on the other end where the inlet valve was closed and the overflow valve was open. If flow was desired in the opposite direction all valves positions were reversed. Open-tube piezometers were used to measure the head in the plenum at either end of the box.

17. In order to measure flow rates, the overflow pipe protruded through the bottom of a steel cup that had a V-notch cut into its side. A bill was welded to the V-notch, directing the discharge water to fall into containers of known volume for measured periods of time. The overflow cup was mounted on a bracket which slid vertically in a slot to adjust the elevations of water entering or leaving. The cup had a reference scale fixed to one side of the slot and calibrated simultaneously with the piezometer scales by filling the empty box to a known water depth and then setting all of the scales to the same reading. The bottom of the box was defined as zero elevation.

Sample

18. Initially, the samples were either sand or pea gravel in a "flow channel" surrounded by soil. The pea gravel was found later to be too coarse and sand was used exclusively. The grain size analyses for the sand and gravel are shown in Figures 2 and 3, respectively.

19. The samples were formed by placing rigid 1/16-in. x 12-in. x 13-in. steel sheets into parallel grooves in the floor between the plenums. The sheets were placed end to end for the full length of the box. A thin lift of aggregate was placed between the two rows of metal and the soil, loess, placed on the outside of each row of metal sheets. It was important to place the soil outside the sheets for each layer of aggregate in order that support be given to the tin sheets and ensure a

constant 1-ft^2 cross section of sand along the length of the box. A thin filter cloth was placed in front of each plenum, on the floor under the samples, and on both sides with a flap left to cover the top of the sample as a single sheet. After the sample was placed to its full 1-ft depth the metal plates were removed, leaving a sand channel between two soil channels of equal height. Soil overburden was then compacted in place. Figure 4 shows the completed sample configuration.

20. To determine the electric potential caused by the flowing water, probes had to be chosen which would minimize electrical self-potential. Self-potential of probes is caused by galvanic reactions of dissimilar metals in an electrolytic fluid. Probes were designed and tested as follows: a copper wire was placed inside a 1/8-in. OD Tygon tube and an aquarium filter was filled with copper sulfate powder and connected to the tubing (Figure 5). The wire was forced into the filter. The Tygon tubing was filled with a saturated solution of copper sulfate. When pairs of these probes were placed in water, the potential difference between the probes was found to be greater than that expected for streaming potential. The self-induced voltage made these probes useless for measuring streaming potentials.

21. A second type of probe was then designed (Figure 5). The copper wire was replaced by coaxial cable. The cable was stripped back 1/2 in. to expose its center wire with insulation intact. The insulation on the center wire was trimmed back 1/4-in. A piece of silver solder wire 4 in. long was soldered to the 1/4-in. stub of the center wire. A plastic sheath covered all but 1/2 in. of the silver solder at the bottom and extended 1 in. above the coaxial cable splice. The sheath was then filled with silicone sealer and allowed to dry. Two of these cables were made 20 ft long with a coaxial connector attached to an aluminum junction box which linked the two coaxial shields together. The wires were shielded in order to eliminate any stray electric potential in the air. After placing the probe tips in water it was noted the observed stray potentials picked up by the exposed and unshielded central conductors disappeared. Additionally, these electrodes cost very little to make and were more durable than the fragile porous pot electrodes.

Detecting streaming
potential using the box model

22. The depth of compacted soil cover over the flow channel determined the maximum possible hydraulic head to be established by a criterion that the overburden pressure not be exceeded. The hydraulic head was set low at first and increased to maximum head for the following tests. The head differential was controlled by two variables: the elevation of the water in the supply barrel and the elevation of the overflow cup at the discharge end of the box. After several preliminary tests it was concluded that for a series of tests the overflow should remain at a constant elevation and the differential head should be regulated by the water elevation in the supply barrel. After setting the head, 5 to 10 min was allowed for equilibrium before measuring the time required to fill a volumetric container. Three measurements were made of the flow rate and the flow was assumed to be in equilibrium if the times did not vary more than 0.5 sec.

23. After the flow was judged to be stable, five parameters were recorded for each test in a series. First, the three piezometers were read, being (a) the water supply, (b) the north, and (c) the south end of the box. The fourth parameter was that of the elevation of the overflow. The fifth and final measurement was that of the electrical streaming potential measured by a high impedance (greater than 50 megohms) digital multimeter. The differential head was then increased and the measurements repeated until the maximum head was reached or the box flooded with water.

24. One of the main problems encountered in the test was instability in the readings. It was found that the loess soil was piping to the surface and through holes in the box. Because of the changing paths for the flow of water and electrical current the box model was judged a failure as far as this experiment was concerned.

Pipe Flow Model

25. The instability in voltage readings encountered with the box flow model was thought to be caused by multiple water flow channels and electrical current paths. There was concern about stray currents caused by radio, television, and industries as well. The pipe flow model was designed and built to eliminate as many variables as possible.

Pipe model construction

26. To keep variables to a minimum the pipe model was simple. The tubular flow cell was a 4-in. OD, 3-1/16-in. ID PVC pipe 2 ft long. Holes were drilled and tapped for 1-in. water pipe in the center of two PVC caps which covered the ends of the PVC pipe. The same manifolds used on either end of the box model were removed and screwed into the caps of the pipe model; 5-29/32 in. from the center in either direction down the length of the pipe holes were drilled and tapped for 3/8-in. pipe thread. A 3/8-in. hole was drilled through the center and down the entire length of two swaged pressure fittings. A hard plastic sheath 5 in. long and 3/8-in. OD was glued over the probes described in paragraph 21, leaving only the 1/2 in. of electrode tip exposed. The altered ferrule fittings were screwed into the two 3/8-in.-diam holes and the two potential probes could be inserted and removed through these watertight fittings. A cylinder of aluminum wire screen was fabricated to encircle the pipe model and the wire on the coaxial shield was connected to both it and the ground to minimize electrical interference. The pipe model was cradled horizontally in wooden brackets. See Figure 6 for details of the pipe model.

Hydraulic system

27. The water supply plumbing for the pipe model was the same as the water supply for the box model with a few exceptions. The water supply barrel was elevated higher to allow greater pressures in the completely sealed sample container. The heads were read by open-tube piezometers as in the box test.

28. Flow through the two manifolds was similar to that of the box model. The water was supplied from a WES waterline. Water flowed

through a 1-in. water pipe either to the left or right end of the pipe model. The water then flowed through the sample in the pipe and out the overflow. In the pipe model the water flowed through a filter cloth at both ends of the cell. The water entered the pipe model, passed through the first filter, continued through the sample, through the second filter and out of the pipe, and through the manifold to the overflow at the opposite end.

Test procedure

29. Measured data were: supply head, discharge water temperature, time of the reading, three separate volume-per-unit time measurements, specimen electrical resistance, probe 1-to-ground voltage, and probe 2-to-ground voltage.

30. The typical test procedure described will be that used for the sand specimen. The pipe model was removed from its cradle and both caps removed. A filter was placed in one of the caps and the cap put back in place over the end of the pipe. The open end of the pipe was held up to the vertical position. Lifts of 4 in. each were placed in the pipe and the pipe vibrated to make the sand more dense or compacted. This procedure was continued until the pipe was completely full and the sand molded to fit inside the other cap. A filter cloth was placed in the other cap and it was placed on the end of the pipe. The probes were inserted and sealed to the pipe and the cylindrical screen shield placed around the pipe. The pipe was placed back in the cradle and the water pipes connected. The same procedure was followed for the crushed limestone tests and the test using sand and soil together.

31. With the supply set at a desired head the valves were set to allow water to flow from left to right, for example, and the time and temperature recorded. As water began to flow from the barrel, the water supply was regulated to maintain a constant water level in the barrel. After the water level was regulated the flow was checked using precision volumetric flasks and timed intervals. Flow tests were repeated until two successive measurements agreed within 0.5 sec after which three recorded flow measurements were made and averaged. The electrical resistance of the water was read by a 1000-Hz ohmmeter through the two

electrodes on the center line of the model cell. Voltage 1 and voltage 2 were then recorded between the probe on the right end of the pipe and a ground wire and the voltage between the probe on the left end of the pipe and a ground wire, respectively. Both of the voltages were read by the digital multimeter.

32. The minimum head in feet observed by trial and error to be capable of maintaining constant flow was subtracted from the maximum head that the system was capable of providing and this number divided in order to have ten tests increasing by equal increments. These ten tests constituted a series of tests after completion of which the direction of flow was reversed and another series of tests performed. After a series of tests in each directions, a different sample was prepared.

PART III: RESULTS

Electrode Testing and Evaluation

33. The initial attempts at developing electrodes were based upon recommendations given in Ogilvy et al. (1969), in Jakosky (1950), and other references. Without exception, the recommended electrode type for any electrical potential survey was the "porous pot" electrode. Electrical connection in such an electrode is made by means of a metallic electrode immersed in an aqueous solution fully saturated with a salt of that electrode metal. The electrolyte is contained in a porous nonmetallic vessel which is, in turn, fully saturated with the electrolyte solution. The porous pot is placed in contact with the ground and the entire assembly is treated as the measuring electrode. The intent of using porous pot electrodes is to minimize galvanic and electrolytic polarization potentials generated by contact of dissimilar metals, dissimilar solutions, or metal-to-soil contact.

34. The porous pot electrodes, intended to be electrically nonpolarizing, were assembled in pairs and tested by using a high-impedance (50 megohm) digital multimeter between the two electrodes while they were immersed in a bath of tap water, which would be the fluid used in the streaming potential tests. Each pair tested was left immersed in the water bath for at least 24 hr before the self-generated electrical potential was measured between them. The immersion period was intended to allow temperatures and osmotic pressure gradients to stabilize. An immediate potential difference between tested electrode pairs of +12 to -60 mv was measured. Of the six electrodes fabricated, all combinations of pairs tested demonstrated the excessive self-potential. The stabilization period was varied between 5 min before measurement and 48 hr but the immediate self-potential values showed no correlatable pattern in magnitude or electrical sign. A pair of electrodes was observed continuously by voltage measurement for a period of 4 hr. The potential varied from +12 mv to +134 mv after 30 min and then decreased to +39 mv in the next 2 hr. The potential had risen again to +73 mv when the series

of measurements was halted. Despite provision of continuous electrolyte replenishment, constant temperature control, and electrical connection quality checks, the porous pot electrodes as constructed and tested never demonstrated electrical stability.

35. Bare silver wire electrodes were used as an expedient control test to differentiate between the effects of using tap water as the measurement fluid and possible electrical instabilities inherent to the porous pot electrodes as constructed. Silver was chosen because it was readily available in the form of silver solder and because it is relatively inert in aqueous solutions as compared to copper or lead. In the first attempt to use the silver electrodes the generated self-potential between them in fresh tap water was found to vary slowly between -3.2 and +3.0 mv over a period of 2 hr. Repetitions of the measurement series, each time using fresh tap water and polished electrodes, confirmed the observed electrical stability of the silver wire electrodes.

36. Cooper et al. (1982) reported successful usage of long copper-clad steel electrodes in the Gathright Dam streaming potential survey. Butler et al. (1981) reported similar success in using 2-ft-long copper electrodes at Clearwater Dam. Based on the above-described field evidence and this study's finding that minimal electrical self-potential was generated by metallic electrodes, the further use of porous pot electrodes was discontinued for this study. No hypotheses are presently offered to explain the successful usage of metallic electrodes nor the instability of the porous pot electrodes as fabricated. During the work with the flow models the efficacy of using metallic electrodes was thought to be fortuitous rather than possibly serendipitous.

Large Parallelepiped (Box) Flow Model

37. A large aboveground model of a soil-confined granular flow channel was constructed as described in paragraph 13. The flow channel was a parallelepiped with flow along the longest dimension. The granular medium was placed in successive lifts of approximately 2 in. to a final depth of 12 in. concurrently with placement of the loess soil

confinement on either side of the channel. The silver wire electrodes were placed by hand as the granular medium and soil lifts were compacted. The electrodes were each located centrally within the square cross section of the flow channel and 1 ft from the nearest respective water distribution plenum. After completing the placement of the granular flow medium further increments of loess soil were compacted in 2-in. lifts over the flow channel and soil lateral confinements. The granular flow medium first placed in the above manner was washed pea gravel of which 90 percent passed a 3/8-in. screen and 98 percent was retained on a No. 4 screen. The gravel was chosen because its intergranular pore space dimension (assumed to be approximately 0.25 in.) was comparable to fracture apertures in jointed rock masses. Gravel was also readily available. The water supply constant head control was set to coincide with the elevation of the top of the flow channel and the system allowed to saturate with water by gravity flow for 24 hr. Open-tube piezometers at either end of the flow channel and in the center verified that the flow channel had a zero gradient along its entire length and the water level in the flow channel was at the top of the channel. The tailwater elevation control was set at 1.010 ft and the headwater elevation control set at 1.020 ft for a gradient of 0.010 ft in 11 ft of length (i = 0.010/11.0 = 0.0009, where i is the gradient). The discharge rate was measured by timing the rate of filling of a 0.270-gal container. The average elapsed time for three successive measurements was 1.577 min and the resultant discharge rate was

$$Q = \frac{\text{Discharge Volume}}{\text{Elapsed Time}} = 0.1712 \text{ gpm}$$

Using Darcy's law for flow through porous media

$$Q = k\ i\ A \tag{2}$$

where

Q = discharge rate (L^3/T)

k = coefficient of permeability to water (L/T)

i = pressure gradient = $\Delta H/\ell$ (L/L)

ΔH = head difference = headwater elev - tailwater elev (L)

ℓ = length of parallelepiped flow channel (L)

A = cross-sectional area of parallelepiped (L^2)

Rearranging gives

$$k = \frac{Q}{iA}$$

and using the above values,

$$k = 190.2 \text{ gpm/ft}^2$$

$$= 12.91 \text{ cm/sec}$$

This value of coefficient of permeability from measured values led to the calculation of Darcy velocity from

$$v = k\, i \qquad (3)$$

where

v = Darcy velocity of flow through a parallelepiped of porous material (L/T)

$v = (12.91)(0.0009)$

$= 0.0116$ cm/sec

and subsequent insertion in the equation for Reynolds number to characterize the flow as laminar or turbulent (Bouwer 1978):

$$N_R = \frac{\gamma_w\, v\, D_{50}}{\mu} \qquad (4)$$

where

N_R = Reynolds number (dimensionless)

γ_w = density of water at 20°C (M/L^3)

D_{50} = average particle size (L)

μ = viscosity of water at 20°C (M/LT)

$$N_R = \frac{(0.9982)(0.0116)(0.635)}{0.010}$$

$$= 0.735$$

Using $N_R < 1.0$ as a criterion for laminar flow (Bouwer 1978), the flow in gravel at a head of 0.01 ft was laminar. Further calculation using Equations 3 and 4 shows, however, that the criterion on Reynolds number would be violated at imposed head differences greater than 0.013 ft. Despite the prediction a test using a head difference of 0.1 ft was performed. The test failed due to piping and flushing out of the loess cover and side constraints. Potential measurements were erratic with variations exceeding 1000 mv. The gravel channel medium was discarded.

38. Washed concrete sand was used next for a granular flow medium in the large flow model. By visual inspection the sand was at least 90 percent quartz grains. The average grain diameter (D_{50}) was 0.0165 in. The gradation was as follows:

Sieve size	Cumulative percent weight retained
No. 4	7.3
No. 8	16.4
No. 16	22.8
No. 30	31.2
No. 50	86.7
No. 100	96.4
No. 200	97.3
Pan	100.0

Assembly of the flow model was as described above for the gravel medium except that a single layer of filter cloth was placed on both sides and top of the soil-encased flow channel to retard soil erosion under high-flow velocities.

39. Water was allowed to flow freely into the buried sand channel under gravity head equal to the elevation of the top of the sand channel. The time required for the central open-tube piezometer to indicate a constant water level along the sand channel was 48 hr. The tailwater

elevation control was left stationary and level with the top of the channel, while the headwater elevation control was raised in 0.1-ft increments at intervals of 1 hr. A head difference of 0.4 ft of water was required before the first water began to flow from the tailwater discharge pipe. The discharge rates varied erratically for several hours before stabilizing at 8 ml/min measured in a graduated cylinder (Q = 0.0021 gpm). Using a gradient of $i = 0.40 \text{ ft}/11.0 \text{ ft} = 0.0364$ and Equation 2, the coefficient of permeability to water was $k = 0.0577 \text{ gpm/ft}^2$ ($= 3.9 \times 10^{-3} \text{ cm}^3/\text{sec}/\text{cm}^2$). The Darcy velocity from Equation 3 was

$$v = 0.0014 \text{ cm/sec}$$

The Reynolds number from Equation 4 was

$$N_R = 0.0009 \ll 1$$

and laminar flow was seen to be probable for all proposed applied pressure heads, thus satisfying a requirement for streaming potential development.

40. The digital multimeter was connected to each of the buried electrodes in turn and the reference ground potential point in the soil outside the model. The reference ground point was not moved as attempts were made to measure generated electric potentials at the electrodes. All successive measurements and observations made on a continuous basis for several minutes varied randomly through a range of about 10 mv with either positive or negative signs. It was reasoned that an electrolytic equilibrium or flow equilibrium had not been achieved, and the system was left in a constant flow condition for three days. During that time the measured electric potentials did not increase or stabilize. The flow of water gradually decreased to a zero rate despite verification of the water supply pressure. To reestablish water flow the headwater elevation control was raised in increments of 0.1 ft from $\Delta H = 0.4$ ft. When the head differential approached 1.0 ft, water was flowing from the

tailwater discharge but the soil encasing the flow channel exhibited signs of complete saturation, heaving and cracking of its surface, and ultimately the surface became covered by water seeping upward. The silicone-caulked joints of the box began leaking and the test was halted without any meaningful electrical data nor establishment of reliably controlled water flow.

41. The conclusion was that the model concept of encasing a fairly large aggregate flow channel in remolded soil was not feasible within the constraints imposed by economical model assembly. Despite the failure to accomplish a detailed series of electric streaming potential measurements the initial data obtained before model failure showed that any measurable streaming potentials were substantially lower in magnitude than random electrical noise levels of $\pm$10 mv. Measurements were made of the electrical resistivity of the water discharged from the model, the resistivity of the sand aggregate saturated with discharged water, and the resistivity of the soil from the model saturated with discharged water. The resistivities were measured using a Lucite cell with dimensions such that a direct measurement of electrical resistance through the tested medium is numerically equal to the electrical resistivity in units of ohm-cm. The resistivities were measured on five samples of each medium and the average values were as follows:

Material	Average electrical resistivity, ohm-cm
Discharge water	5,300
Saturated sand	50,500
Saturated soil	2,875

From the CRC Handbook of Chemistry and Physics (Weast, Selby, and Hodgman 1965) the dielectric constant of water at 20°C, D, equals 80.36. From Mandal (1969) the surface potential, ζ_s, or zeta potential for sand and tap water equals -1250 mv. The fluid electrical conductivity is obtained as the inverse of the fluid electrical resistivity:

$$K_{f1} = \frac{1}{\zeta_{f1}} \tag{5}$$

where

ζ_{fl} = fluid electrical resistivity (ohm-cm)

Equation 1 is stated in terms of electrostatic units of potential and centimetres head of water. To convert to the centimetre-gram-second system of measures the following factors are applied:

$$\frac{\Delta E}{P} = D_{fl} \quad \zeta_s / 4\pi \mu K_{fl} \qquad (1 \text{ bis})$$

$$= \frac{D_{fl} \zeta_s \left(\frac{1}{8.99 \times 10^{11}}\right) g}{4\pi \frac{\mu}{\gamma_{fl}} K} \qquad (6)$$

where

g = gravitational acceleration = 980 cm/sec^2

γ_{fl} = density of water at 20°C = 0.999 $gram/cm^3$

Inserting values for the soil-enclosed sand channel,

$$\frac{\Delta E}{P} = \frac{(80.37)(-1250)\left(\frac{1}{8.99 \times 10^{11}}\right) \quad (980)}{4\pi \left(\frac{0.01}{0.999}\right)\left(\frac{1}{5300}\right)}$$

$$= 4.61 \text{ mv/cm}$$

And for P = 12.92 cm water

ΔE = -59.6 mv

42. The calculated magnitude for streaming potential, 59.6 mv, is higher by a factor of 6 than the variations actually observed in the model test. A possible cause of the measurement failure was determined to be electrical in nature by conceptualizing the model flow channel as an electrical battery with one pole at the inserted electrode and the other at the common grounding point outside the model. The extremely low resistivity of the saturated soil compared to that of the saturated sand (2,875 ohm-cm compared to 50,500 ohm-cm) provides a possible current path between all portions of the channel periphery through the saturated soil and wood to the grounding point and essentially

"short-circuits" any developed streaming potential. A second possible cause of measurement failure lies within the electrochemical behavior of clay minerals, specifically that generated streaming potentials are positive in sign and thus opposite to those generated in silica aggregates. The loess soil used in the model contains 10-15 percent clay; water was observed to flow macroscopically out of the soil and is assumed to also flow microscopically in the pore spaces of the soil. The addition of positive clay-generated streaming potentials to negative sand-generated streaming potentials effectively could degrade measurements completely.

Plastic Tube (Pipe) Flow Model

43. Because of failure to control water flow in a satisfactory way and to measure meaningful streaming potentials in the large above-ground parallelepiped model a test cell was fabricated from PVC plastic pipe as described in paragraph 26. The granular flow media was packed into the cylindrical cell, densified by impact, electrodes inserted, and the cell was sealed and attached to the same head and tailwater elevation controls as for the larger test. The test cell consistently allowed control of the pressure gradient to within 0.01 ft over its 2-1/2-ft length. The discharge rates varied uncontrollably twice in the entire sequence of testing due to clogging of the filter cloth at the discharge and twice because incomplete densification prior to flow initiation caused a longitudinal void to develop during flow of water. The tests in which discharge rates varied uncontrollably were each reconstructed and performed again.

44. Temperature measurements were made in the discharged water during each test for use in determining the dielectric constant variation and the water density variation. The temperature extremes measured were a low of 17°C and a high of 30.5°C. Corresponding values of the dielectric constant are 81.47 and 76.58 (an inverse linear variation of 6 percent). Corresponding variations of water density were from 0.9988 g/cm^3 to 0.9955 g/cm^3 (an inverse nonlinear variation of 0.3 percent). Both corrections for temperature-induced variations were included in the ensuing data reduction.

45. The resistivity of the water used in the tests was expected to vary both with changes in temperature and with changes in the municipal water treatment. The temperature dependence of an aqueous electrolyte is stated as (Keller and Frischknecht 1966):

$$\rho_t = \frac{\rho_{to}}{1 + 0.025\ (t - t_o)} \tag{7}$$

where

ρ_t = resistivity at the ambient temperature, t (ohm-cm)

ρ_{to} = resistivity at a reference temperature, t_o (ohm-cm)

t = ambient temperature (deg C)

t_o = reference temperature (deg C)

Variations in the electrical resistivity of the tap water used for the streaming potential tests were essentially uncontrollable but could be monitored periodically through each test. The method was to use the plastic flow test cell as a resistivity measurement cell. The electrodes implanted in the cell and aggregate for measuring streaming potential were used as electrical resistance measurement electrodes alternately with their primary function. To convert electrical resistance measurements between the electrodes into fluid resistivity data a cell constant was determined by use of the unit resistivity cell described in paragraph 42. Tap water at 20°C was placed in the unit cell and the resistivity measured. Clean sand was then packed into the unit cell as firmly as possible and the resistivity of the tap water saturated sand measured to provide an adjustment factor for relating fluid resistivity to fluid-saturated sand resistivity. Sand from the same source was then packed into the flow model cell to the same degree of firmness as in the unit resistivity cell, determined by finger penetration effort. The flow model cell was then saturated with 20°C water by means of the fabricated controlled-headwater supply. An electrical resistance measurement across the imbedded electrodes was then made. Because the manual compaction of the aggregate into the flow model cell in all further tests was made as similar in effort as possible and because the physical configuration of the flow model cell was not altered, it was assumed

that any variations in measured electrical resistance were directly proportional to changes in the fluid resistivity. Incorporating both the water-to-saturated sand resistivity cell factor and the resistivity cell-to-flow model cell factor, the empirical relationship

$$\rho_{fl} = 0.163\ R \tag{8}$$

where

R = measured electrical resistance (ohms)

was used for all further fluid resistivity determinations.

46. Figure 7 is a plot of all calculated fluid resistivities versus temperature. The points are grouped according to the day of testing in which the data were obtained. Also included is a plot based on Equation 7 using 20°C and 5300 ohm-cm as the reference temperature and fluid resistivity, respectively. There is a slight tendency for the resistivity versus temperature data to follow the theoretical curve, but the scatter is extreme among different days of testing. Variations in the ion content of the tap water from day to day of the magnitude indicated by the resistivity changes are possible within the standards of the Public Health Service. The resistivity extremes of about 1500-6000 ohm-cm observed can be interpreted (OCE 1979) as caused by a dissolved ion content range of 75-350 mg/l equivalents of NaCl. The maximum desired content of chloride in drinking water is 250 mg/l and of total dissolved solids is 500 mg/l (Bouwer 1978). The final conclusion was that fluid electrical resistivity varied to such a degree that the streaming potential measurements had to be directly coupled to resistivity measurements and temperature corrections were of relatively much less importance.

47. Flow media tested for streaming potential were:

a. Washed concrete sand (primarily quartz).

b. Washed pea gravel (primarily silica chert).

c. Washed crushed limestone sand.

d. Washed limestone gravel.

e. Washed concrete sand over loess soil.

The washed concrete sand medium was as described in paragraphs 18 and 39 for the large parallelepiped model as was the washed pea gravel (paragraphs 18 and 38). The limestone sand was crushed and wet-sieved specifically for the present test series. It was packed into the flow model cell in the same manner as the concrete sand. The limestone gravel was obtained from a bulk stockpile called "crushed limestone rock" and washed prior to placing in the flow model cell. To examine the conditions in the earlier large parallelepiped model which failed, the final test in the tubular cell consisted of a compacted layer of loess soil placed longitudinally with the remaining 25 percent of the circular cross section filled with compacted concrete sand.

48. Tabulated results of the above described tests are presented in Tables 1-5. Plots of measured streaming potentials versus water pressure differential are presented in Figures 8-12. Calculations were made to determine the electric surface potential (zeta potential) for each measurement. Those surface potentials are plotted versus water flow rate in Figures 13-17.

49. The plots of streaming potential, ΔE_{sp}, versus applied differential pressure, P, show that little direct variation in streaming potential was observed as related to changes in pressure. In any given series of measurements with a particular flow medium in one direction the measured streaming potential was essentially constant as pressure changed. In all the measurements taken as a whole the streaming potential varied between -200 mv and -360 mv with a range of differential pressure variation between 39 cm of water and 108 cm of water.

50. The plots of surface potential, ζ_s, versus volume flow rate, Q, show relationships that appear to be hyperbolic with one asymptote parallel to an upper constant surface potential value that is characteristic of the flow media and the other asymptote parallel to a low magnitude constant volume flow rate. The data were not, however, adequately controlled to justify regression to empirical equations relating surface potential to flow rate.

PART IV: CONCLUSIONS AND RECOMMENDATIONS

Conclusions

51. This study of modeling electrokinesis phenomena by measuring electrical streaming potentials in realistic geologic media has produced a number of observations that do not agree with past studies of electrokinesis. The conclusion reached early in the activities of fabricating flow models using naturally occurring granular and soil materials was that composite models for confined flow channels are difficult to assemble with sufficient control to allow precise electrokinetic measurements. Specific problems were identified as the inability to establish and maintain a uniform flow of water, the imperfect confinement of the water within the aggregate channels both hydraulically and mechanically, and the impossibility of electrically isolating the flowing water from the surrounding clay-bearing soil.

52. Despite recommendations of earlier investigators that the only type of electrode appropriate to measure streaming potentials was a low self-polarizing porous pot electrode, it was found in this study that inert metal (silver) electrodes were far more stable electrically than were the specially fabricated porous pot electrodes. The use of metallic electrodes has also proven to be successful in field applications by the EEGD independently of this study. In addition to demonstrated electrical stability the metallic electrodes were found to be more economical to fabricate and are more durable.

53. Electrical potentials were measured in the modeled systems of water flowing through porous media. Electrical potentials measured in media that included water at rest were of much lower magnitude (-250 mv compared to $\pm$3 mv) and were interpreted as being electrical "noise." Therefore, the measured electrical potentials in flowing water are interpreted as successful detection of the electrokinetic phenomenon, despite the poor correlation with the theoretical predictions of Equation 1 and other investigators. No correlation of streaming potential data to the lithology of the aggregate in the flow channels was found. All

measured streaming potentials were negative in electrical sign and were of reasonable magnitudes, but they showed insufficient variation because of applied pressure differential to justify direct comparison to the theoretical relationships as determined under controlled laboratory conditions. The magnitude of streaming potentials was strongly influenced by the electrical resistivity of the water used. The effect of resistivity was stronger than could be accounted for by temperature changes. Variations in the dissolved ionic content of the water were determined to be the primary uncontrolled variable. Both the dielectric constant and the viscosity of the water vary with temperature and play a part in influencing streaming potential magnitudes but to a substantially lesser degree than the chemistry effect of dissolved ions does by way of electrical fluid resistivity.

54. To accommodate uncontrolled electrical resistivity variations, measurements of resistivity were made in conjunction with measurements of streaming potential. Thus variations in the grain surface potential during water flow could be determined by calculation. The surface potential was found to vary by an approximate hyperbolic relationship with measured volume flow rates. The surface potential was found to be in the range from -0.5 to -2.5 volts for quartz sand and sand over soil, between -1.0 and -3.0 volts for limestone sand, between -2.0 and -2.5 volts for limestone gravel, and between -2.0 and -6.5 volts for silica chert pea gravel. A relationship between surface potential and volume flow rate has not previously been described in the literature, though regular variations in surface potential caused by duration of flow have been described by Mandal (1969).

Recommendations

55. Further studies defining electrokinetic phenomena and developing streaming potential surveys should be performed in real geologic environments rather than modeled geologic conditions. Very close control on ancillary measurements of electrical resistivity, temperature, and flow conditions will be required in such field studies, but model

fabrications such as described herein incorporate too many compromises with reality to be satisfactory for simulating actual geologic conditions.

56. Future streaming potential surveys should be used strictly on a developmental basis until there is a better understanding of the factors controlling streaming potentials. Temperature effects are relatively easy to incorporate in streaming potential data reduction as they affect the dielectric constant, the viscosity, and to some degree the fluid resistivity. However, two variables, fluid resistivity as controlled by dissolved ion concentrations and the grain surface potential, demonstrated large unanticipated variations in this study to the extent that measured streaming potentials were largely uncorrelatable. Frequent and accurate fluid resistivity measurements are required for future quantitative applications of streaming potential surveys.

57. Metallic electrodes were found to be acceptable for measuring electrical potentials in earth materials during this study. Porous pot "nonpolarizable" electrodes were found to be unsatisfactory. Previous investigations, with the exception of work by the EEGD, predict exactly the opposite comparative success between the two types of electrode. Further study is recommended to determine the most appropriate electrode type for streaming potential measurements and to explain the reasons for successful use of metallic electrodes in streaming potential studies by the WES.

58. The unexpected observed relationship of grain surface potential with volume flow rate deserves future close attention for two reasons. First, the variability of surface potential adds one more unknown to the quantitative interpretation of streaming potential data. Second, the volume flow rate is related by the flow medium microscopic geometry to the intergranular flow velocity. Verification of the dependence of surface potential on volume flow rate or, by inference, on flow velocity could then make possible the use of streaming potential data to calculate flow velocities in situ rather than be used only as an indicator of the existence of flow or as a differential head measurement technique. That verification is strongly recommended on both a theoretical and experimental basis.

REFERENCES

Bates, E. R. 1973. "Detection of Subsurface Cavities," Miscellaneous Paper S-73-40, U. S. Army Engineer Waterways Experiment Station, CE, Vicksburg, Miss.

Bernstein, F., and Scala, C. 1959. "Some Aspects of the Streaming Potential and the Electrochemical SP in Shales," Petroleum Transactions of the American Institute of Mining Engineers, Vol 216, pp 465-468.

Bogoslovosky, V. A., and Ogilvy, A. A. 1970. "Natural Potential Anomalies As a Quantitative Index of the Rate of Seepage From Water Reservoirs," Geophysical Prospecting, Vol 18, No. 2, pp 261-268.

Bouwer, H. 1978. Groundwater Hydrology, McGraw-Hill, New York.

Bull, H. B., and Gortner, R. A. 1932. "Electrokinetic Potentials. X. The Effect of Particle Size on the Potential," Journal of Physical Chemistry, Vol 36, No. 3, pp 111-119.

Butler, D. K., Llopis, J. L., Koester, J. P., and Kean, T. B. 1981. "Geophysical Surveys, Clearwater Dam, Missouri," Unpublished Report, Geotechnical Laboratory, U. S. Army Engineer Waterways Experiment Station, CE, Vicksburg, Miss.

Cooper, S., Koester, J. P., and Franklin, A. G. 1982. "Geophysical Investigations at Gathright Dam," Miscellaneous Paper GL-82-2, U. S. Army Engineer Waterways Experiment Station, CE, Vicksburg, Miss.

Corson, D., and Lorraine, P. 1962. Introduction to Electromagnetic Fields and Waves, W. H. Freeman and Company, San Francisco.

Department of the Army, Office, Chief of Engineers. 1979. "Geophysical Exploration," Engineer Manual 1110-2-1802, Washington, D. C.

Gondouin, M., and Scala, C. 1958. "Streaming Potential and the SP Log," Journal of Petroleum Technology.

Helmholtz, H. Von. 1951. Annales Physik, No. 3:1879, Gesammelte Abhandlugen, Vol 1, 1882, Transl. P. E. Bocquet, "Two Monographs of Electrokinetics," Eng. Res. Publ. No. 33, University of Michigan, Ann Arbor.

Jakosky, J. J. 1950. Exploration Geophysics, Trija Publishing Company, Los Angeles, Calif.

Keller, G. V., and Frischknecht, F. C. 1966. Electrical Methods in Geophysical Prospecting, Pergamon Press, New York.

Mandal, T. C. 1969. An Electrokinetic Study of Incrustation and Corrosion of Water Well Screen, M.S. Thesis, University of Nebraska, Lincoln, Nebr.

Mandal, T. C., and Edwards, D. M. 1971. "The Effects of Electrokinetics Upon Incrustation in Water Wells," Transactions of the American Society of Civil Engineers, Vol 14, No. 3.

Ogilvy, A. A., Ayed, M. A., and Bogoslovsky, V. A. 1969. "Geophysical Studies of Water Leakages From Reservoirs," Geophysical Prospecting, Vol 17, No. 1, pp 36-62.

Saucier, R. T. 1970. "Geoelectrical Survey Performance and Evaluation, Walter F. George Reservoir, Alabama-Georgia," Miscellaneous Paper S-70-17, U. S. Army Engineer Waterways Experiment Station, CE, Vicksburg, Miss.

Schriever, W., and Bleil, C. E. 1957. "Streaming Potential in Spherically Grained Sands," Journal of the Petrochemical Society, pp 170-175.

Smoluchowski, M. Von. 1951. Electrisch and Streaming Strome Handbuch de Electrizitat und des Magnetismers, Graetz (ed.), Vol II, P. E. Bocquet, "Two Monographs of Electrokinetics," Eng. Res. Publ. No. 33, University of Michigan, Ann Arbor.

Weast, R. C., Selby, S. M., and Hodgman, C. D. 1965. Handbook of Chemistry and Physics, The Chemical Rubber Company, Cleveland, Ohio.

Wyllie, M. R. J. 1951. "An Investigation of the Electrokinetic Component of the Self Potential Curve," Transactions of American Institute of Mining Engineers, Vol 192, pp 1-18.

Table 1

Tubular Cell Streaming Potential Measurements, Quartz Sand

Pressure Differential, cm water	Volume Flow Rate, cm^3 sec	Temperature, deg C	Fluid Resistivity, kilohm-cm	Streaming Potential, negative millivolts	Surface Potential, negative volts
		Flow to Right			
108.30	0.556	25.5	3.831	323.5	1.150
101.44	0.488	27.0	3.749	307.5	1.202
94.58	0.445	25.5	3.831	338.0	1.376
87.72	0.393	26.0	3.831	328.5	1.446
80.86	0.336	26.0	3.831	322.5	1.540
74.01	0.245	19.0	4.320	325.0	1.454
67.15	0.195	20.0	4.156	324.5	1.671
60.29	0.153	19.5	4.059	335.0	1.962
53.43	0.109	20.0	4.059	341.0	2.259
		Flow to Left			
108.30	0.654	23.0	5.738	241.5	0.566
101.44	0.589	24.0	5.705	225.5	0.571
94.58	0.520	25.0	5.705	218.5	0.596
87.72	0.462	24.5	5.705	216.5	0.635
80.86	0.433	25.0	5.738	203.0	0.644
74.01	0.369	26.0	5.738	206.5	0.719
67.15	0.308	26.0	5.738	207.5	0.796
60.29	0.254	26.5	5.738	247.0	1.059
53.43	0.201	27.0	5.738	244.0	1.183
39.72	0.117	27.0	5.705	251.0	1.646

Table 2

Tubular Cell Streaming Potential Measurements, Pea Gravel

Pressure Differential, cm water	Volume Flow Rate, cm^3 sec	Temperature, deg C	Fluid Resistivity, kilohm-cm	Streaming Potential, negative millivolts	Surface Potential, negative volts
		Flow to Right			
108.30	45.58	24.0	1.695	304.5	2.430
101.44	42.47	24.0	1.695	285.0	2.428
94.58	38.42	24.5	1.663	258.0	2.406
87.72	34.85	24.5	1.663	260.5	2.620
80.86	28.19	26.5	1.597	270.0	3.099
74.01	25.64	26.0	1.597	261.5	3.272
67.15	21.99	27.0	1.581	284.0	3.978
60.29	18.87	26.0	1.581	295.5	4.585
53.43	14.22	23.0	1.646	249.5	4.136
39.72	17.97	23.0	1.646	248.0	5.530
		Flow to Left			
108.30	39.87	24.0	1.614	291.0	2.439
101.44	37.71	24.0	1.614	295.5	2.644
94.58	35.23	24.0	1.614	289.0	2.774
87.72	32.39	25.0	1.614	276.5	2.875
80.86	30.18	25.0	1.597	289.5	3.300
74.01	27.75	26.0	1.597	287.5	3.598
67.15	25.42	26.0	1.597	285.0	3.931
60.29	22.53	26.0	1.597	275.5	4.232
53.43	19.31	26.0	1.597	275.0	4.767
39.72	13.34	26.0	1.597	282.5	6.587

Table 3

Tubular Cell Streaming Potential Measurements, Limestone Sand

Pressure Differential, cm water	Volume Flow Rate, cm^3/sec	Temperature, deg C	Fluid Resistivity, kilohm-cm	Streaming Potential, negative millivolts	Surface Potential, negative volts
		Flow to Right			
108.30	6.54	24.0	3.260	266.5	1.106
101.44	5.95	24.0	3.260	357.5	1.584
94.58	5.32	24.0	3.260	353.0	1.677
87.72	4.87	24.0	3.260	259.0	1.327
80.86	4.32	25.0	3.340	260.0	1.417
74.01	3.66	25.0	3.340	258.0	1.536
67.15	3.14	25.0	3.340	259.0	1.700
60.29	2.72	25.5	3.420	258.5	1.849
53.43	2.27	26.0	3.420	260.5	2.109
39.72	1.60	26.0	3.420	261.0	2.842
		Flow to Left			
108.30	5.36	26.0	3.100	312.0	1.374
101.44	4.70	26.0	3.160	282.0	1.301
94.58	4.20	26.0	3.160	283.5	1.403
87.72	3.72	28.0	3.160	282.0	1.520
80.86	3.34	28.0	3.210	283.5	1.632
74.01	2.59	26.0	3.340	303.5	1.816
67.15	2.26	27.0	3.340	320.5	2.125

Table 4

Tubular Cell Streaming Potential Measurements, Limestone Gravel

Pressure Differential, cm water	Volume Flow Rate, cm^3 sec	Temperature, deg C	Fluid Resistivity, kilohm-cm	Streaming Potential, negative millivolts	Surface Potential, negative volts
		Flow to Right			
108.30	67.52	28.0	1.712	280.0	2.256
101.44	55.85	29.5	1.712	246.0	2.131
94.58	37.63	30.5	1.712	241.0	2.251
108.30	39.33	29.0	1.760	279.0	2.197
101.44	33.07	29.0	1.760	255.0	2.144

Table 5

Tubular Cell Streaming Potential Measurements, Sand Over Soil

Pressure Differential, cm water	Volume Flow Rate, cm^3 sec	Temperature, deg C	Fluid Resistivity, kilohm-cm	Streaming Potential, negative millivolts	Surface Potential, negative volts
		Flow to Right			
108.30	0.131	24.0	4.972	238.0	0.647
101.44	0.122	24.5	4.890	211.0	0.625
94.58	0.112	24.0	4.890	218.5	0.692
87.72	0.103	24.0	4.890	218.0	0.746
80.86	0.094	24.0	4.890	217.5	0.805
74.01	0.084	24.0	4.890	241.5	0.977
67.15	0.068	17.0	5.298	329.5	1.312
60.29	0.062	17.0	5.379	302.0	1.319
53.43	0.055	17.0	5.379	292.5	1.442
39.72	0.041	18.0	5.281	273.0	1.851
		Flow to Left			
108.30	0.135	20.0	4.075	302.0	0.984
101.44	0.125	20.0	4.075	298.0	1.035
94.58	0.115	20.0	4.075	308.0	1.149
87.72	0.104	20.0	4.108	317.5	1.267
80.86	0.095	20.0	4.108	321.5	1.391
74.01	0.084	21.0	4.026	307.0	1.488
67.15	0.075	21.0	4.026	311.0	1.661
60.29	0.056	21.5	3.994	298.0	1.791
53.43	0.048	22.0	3.994	303.5	2.064
39.72	0.031	23.0	3.928	290.5	2.715

A - WATER SUPPLY
B - WES WATER LINE
C - *MANIFOLD ON SUPPLY BARREL
D - *MANIFOLD ON NORTH END
E - *MANIFOLD ON SOUTH END
F - SOUTH OVERFLOW AND SCALE
G - NORTH OVERFLOW AND SCALE
H - PIEZOMETERS
I - SUPPORT ABOUT THE VERTICAL AXIS
J - SUPPORT ABOUT THE HORIZONTAL AXIS
K - COAXIAL CABLE LEADING TO PROBE
L - MULTIMETER
M - ALUMINUM JUNCTION BOX
N - GRADED GROUND LEVEL

* - THESE MANIFOLDS CONSIST OF TWO VALVES AND OTHER PIPE FITTINGS

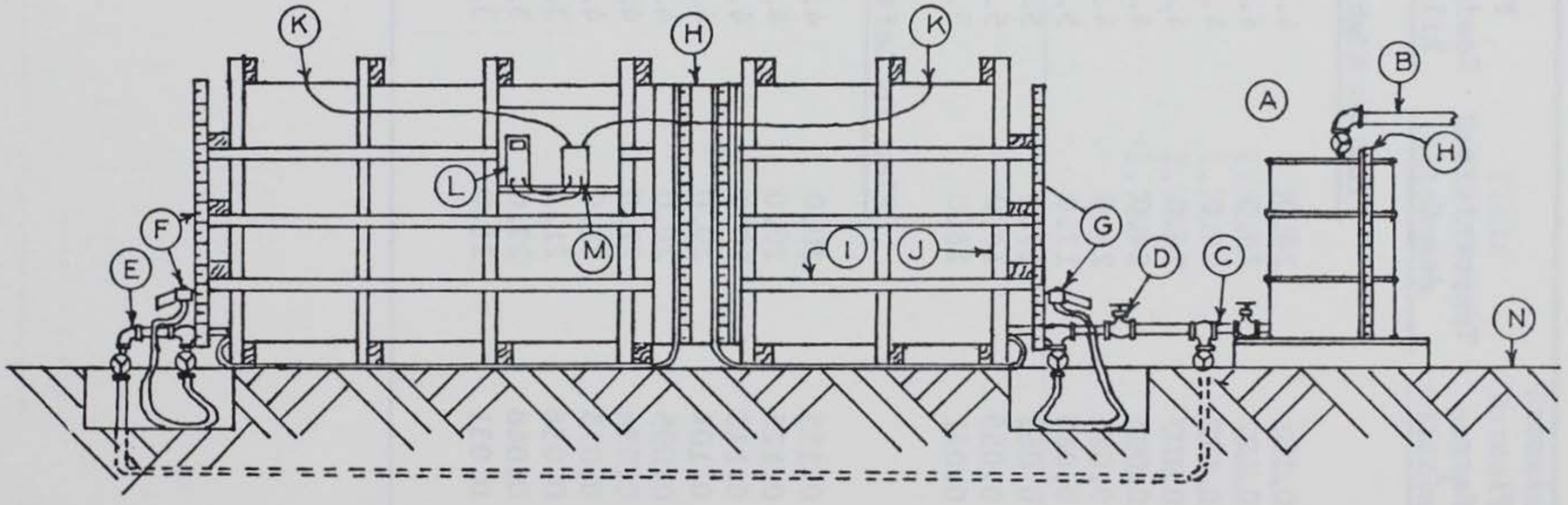

Figure 1. Box model

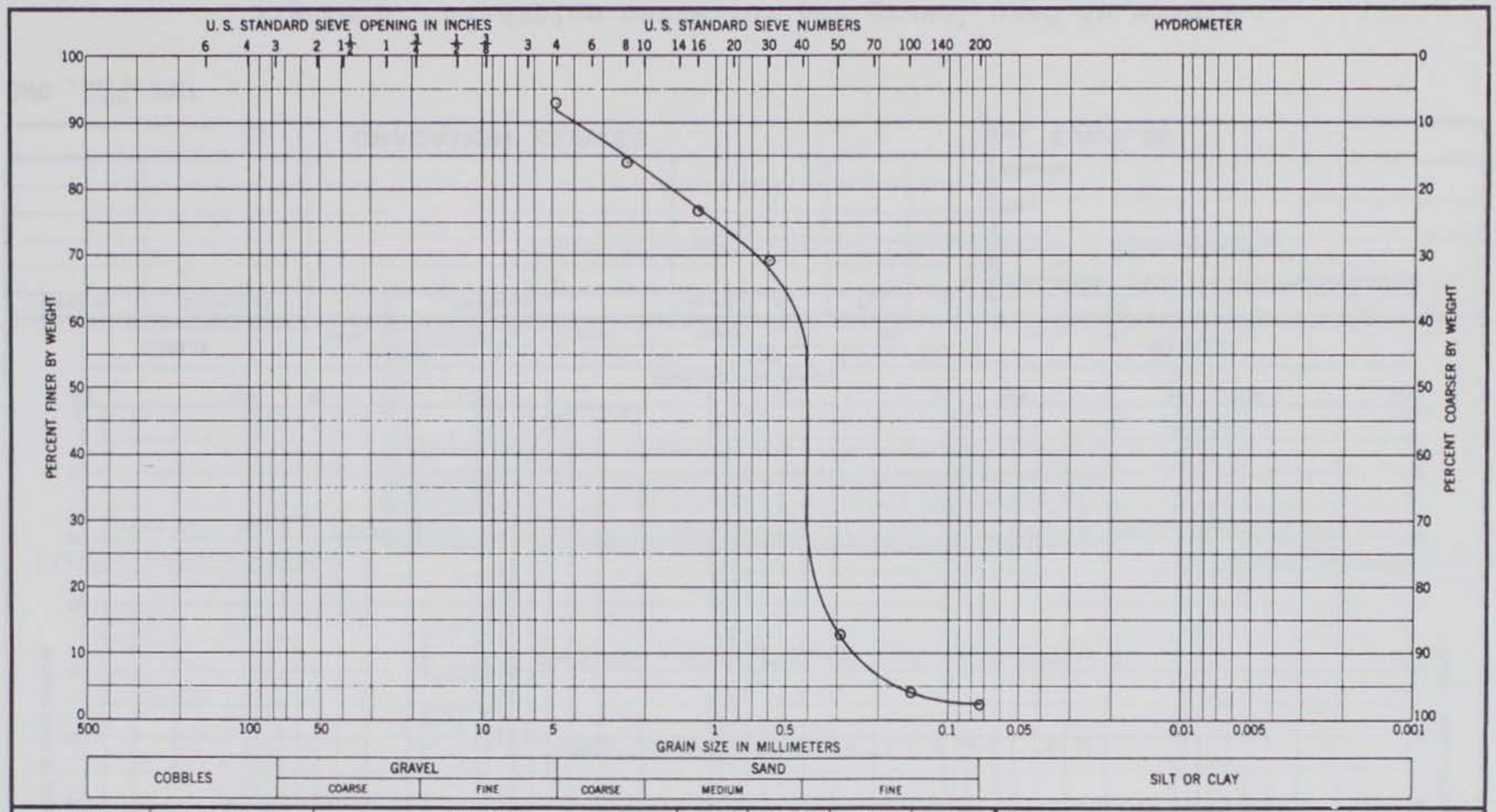

Sample No.	Elev or Depth	Classification	Nat w %	LL	PL	PI

GRADATION CURVES

Project ELECTROKINESIS MODELING
"CONCRETE SAND"
~~Area~~
~~Boring No.~~
Date 23 JAN 81

ENG FORM 1 MAY 63 2087

Figure 2. Gradation curve for sand used in models

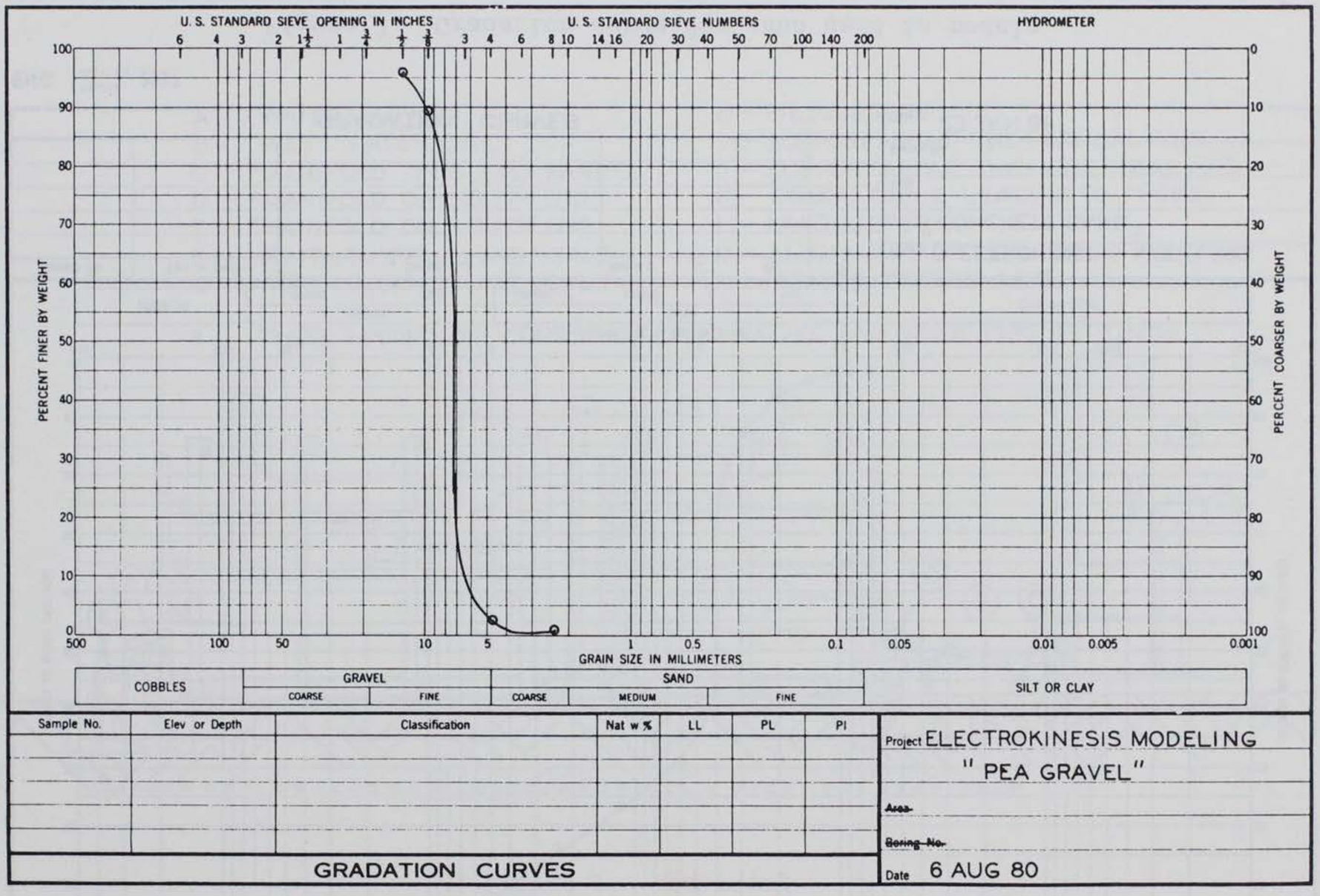

Figure 3. Gradation curve for pea gravel used in models

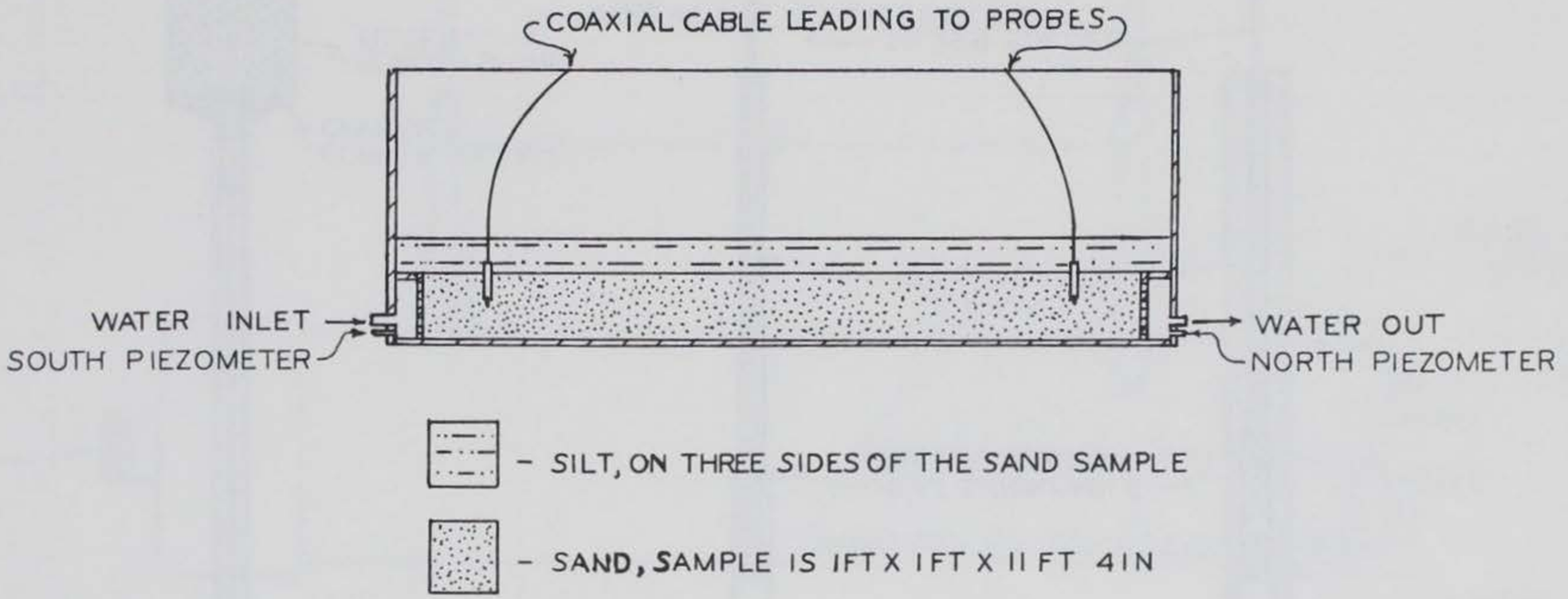

Figure 4. Box model, cross section

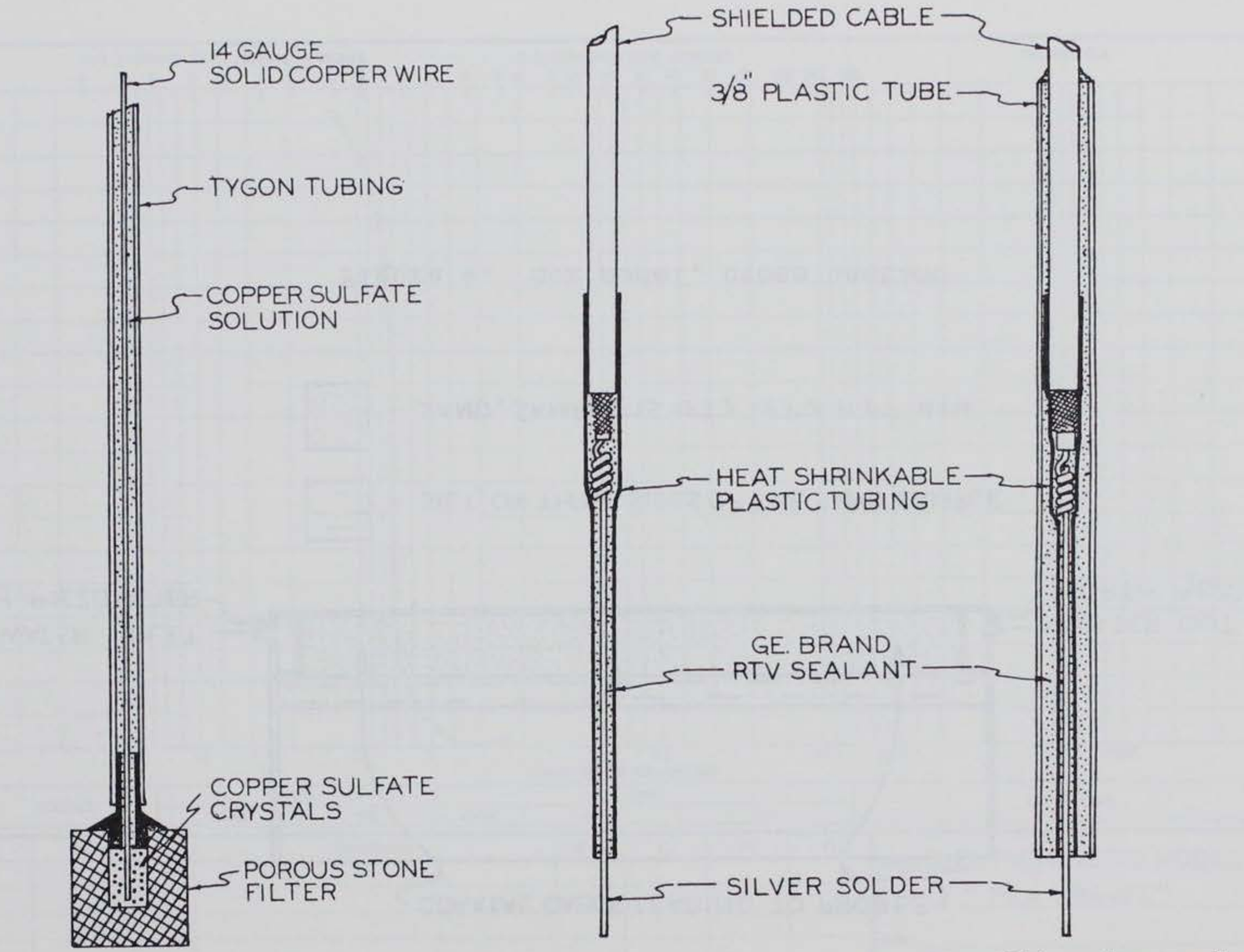

a. Porous pot electrode

b. Metallic electrode used in box model

c. Metallic electrode used in tube model

Figure 5. Electrodes used for electrokinesis modeling

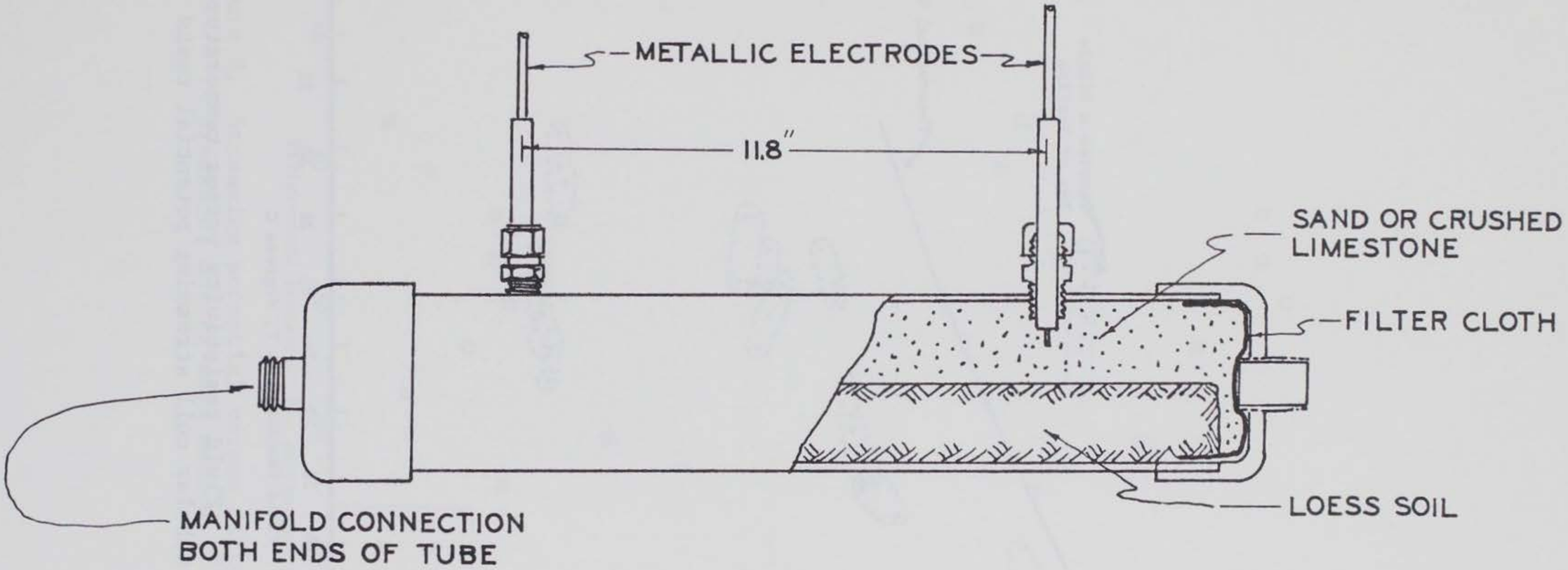

Figure 6. Tube (pipe) model

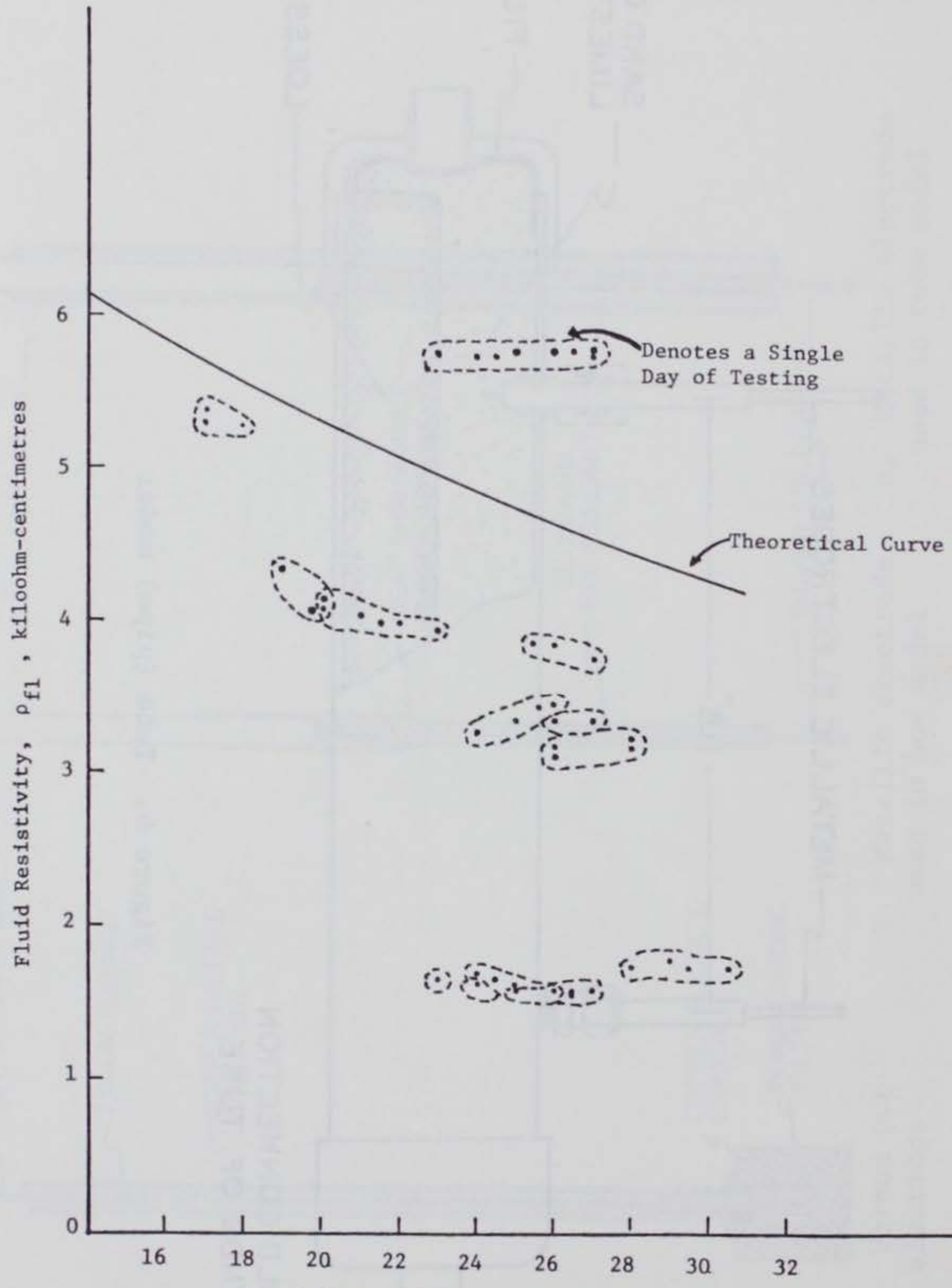

Figure 7. Fluid resistivity versus temperature, all tubular cell streaming potential tests

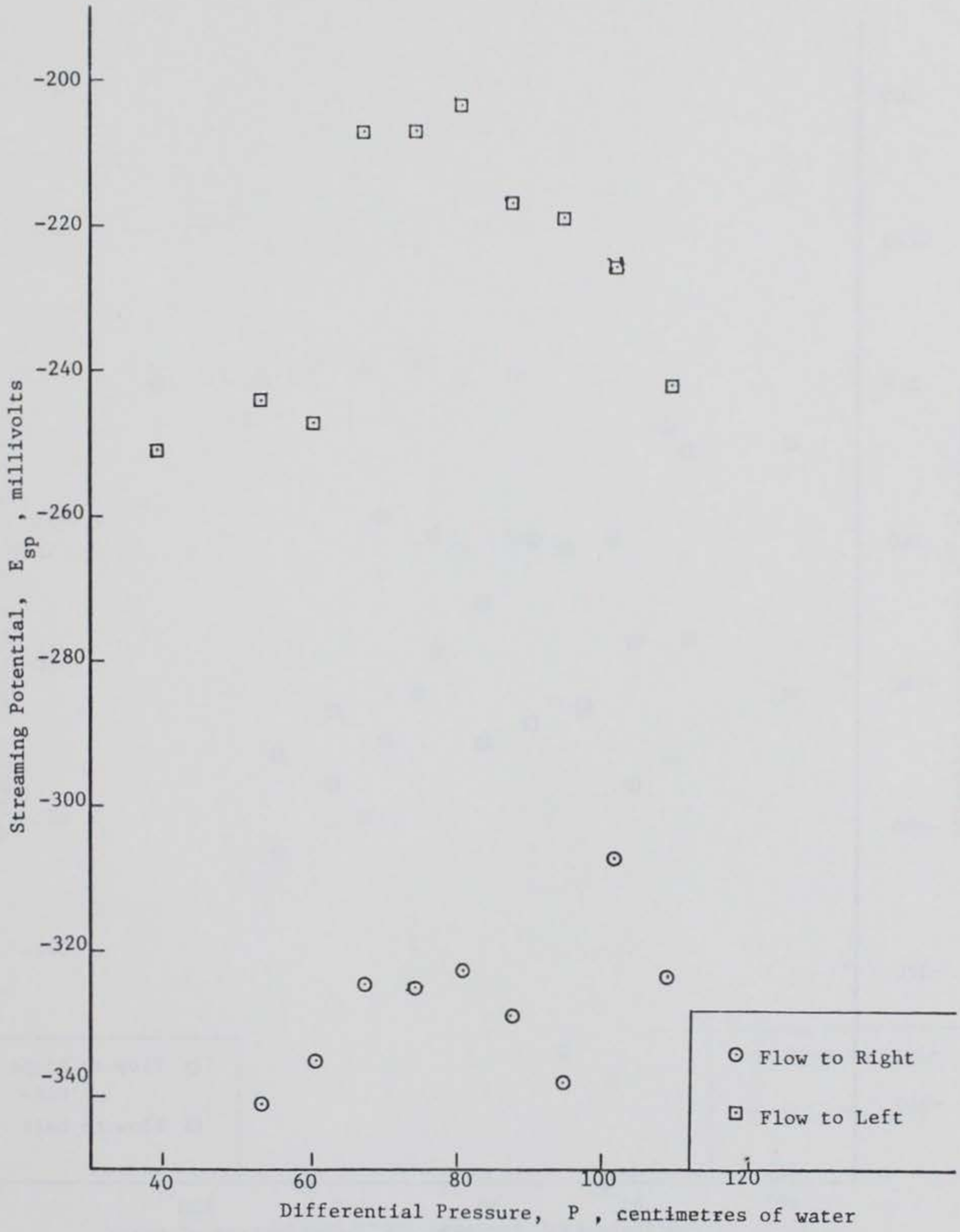

Figure 8. Streaming potential versus differential pressure, quartz sand medium

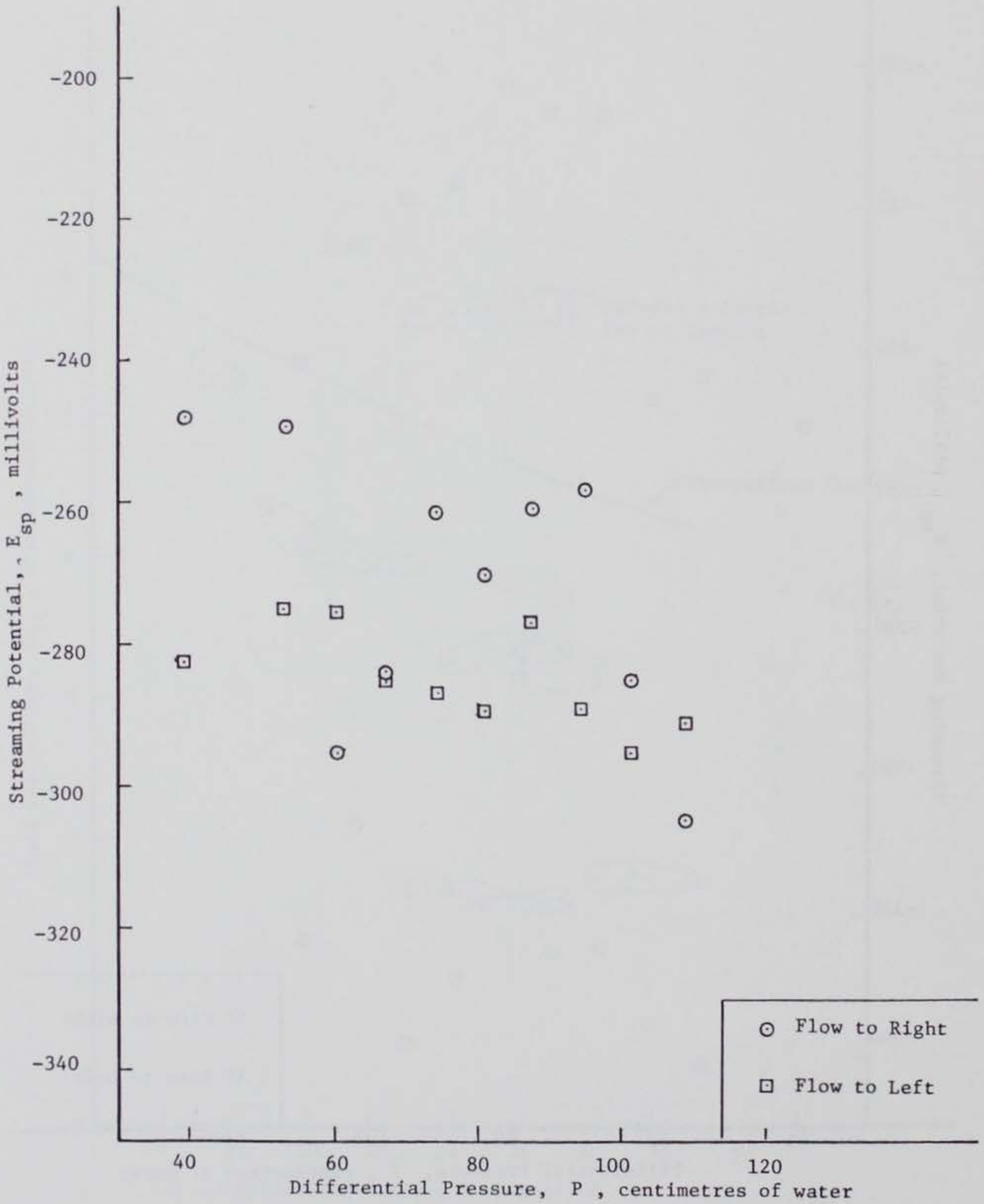

Figure 9. Streaming potential versus differential pressure, chert pea gravel medium

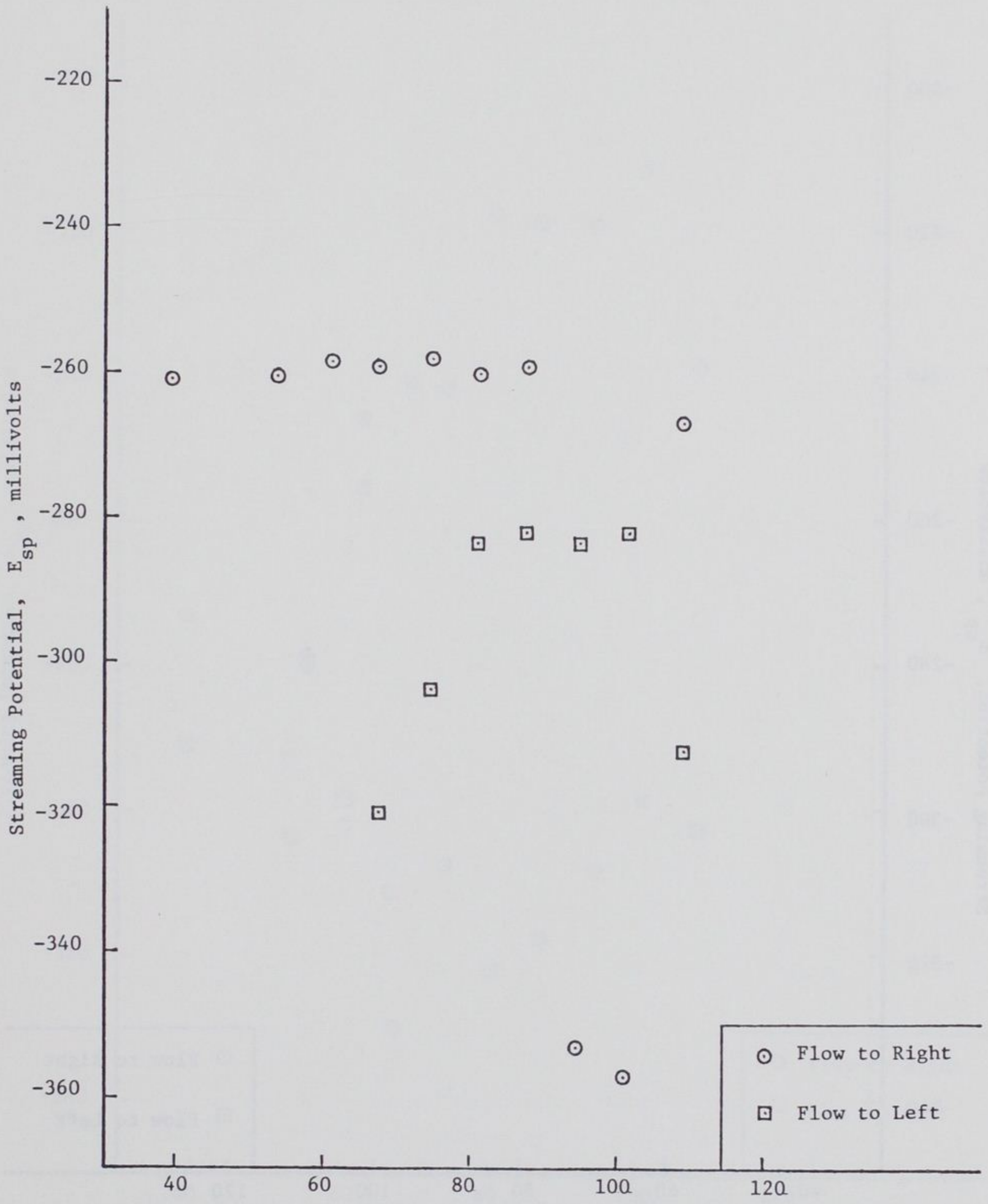

Figure 10. Streaming potential versus differential pressure, limestone sand medium

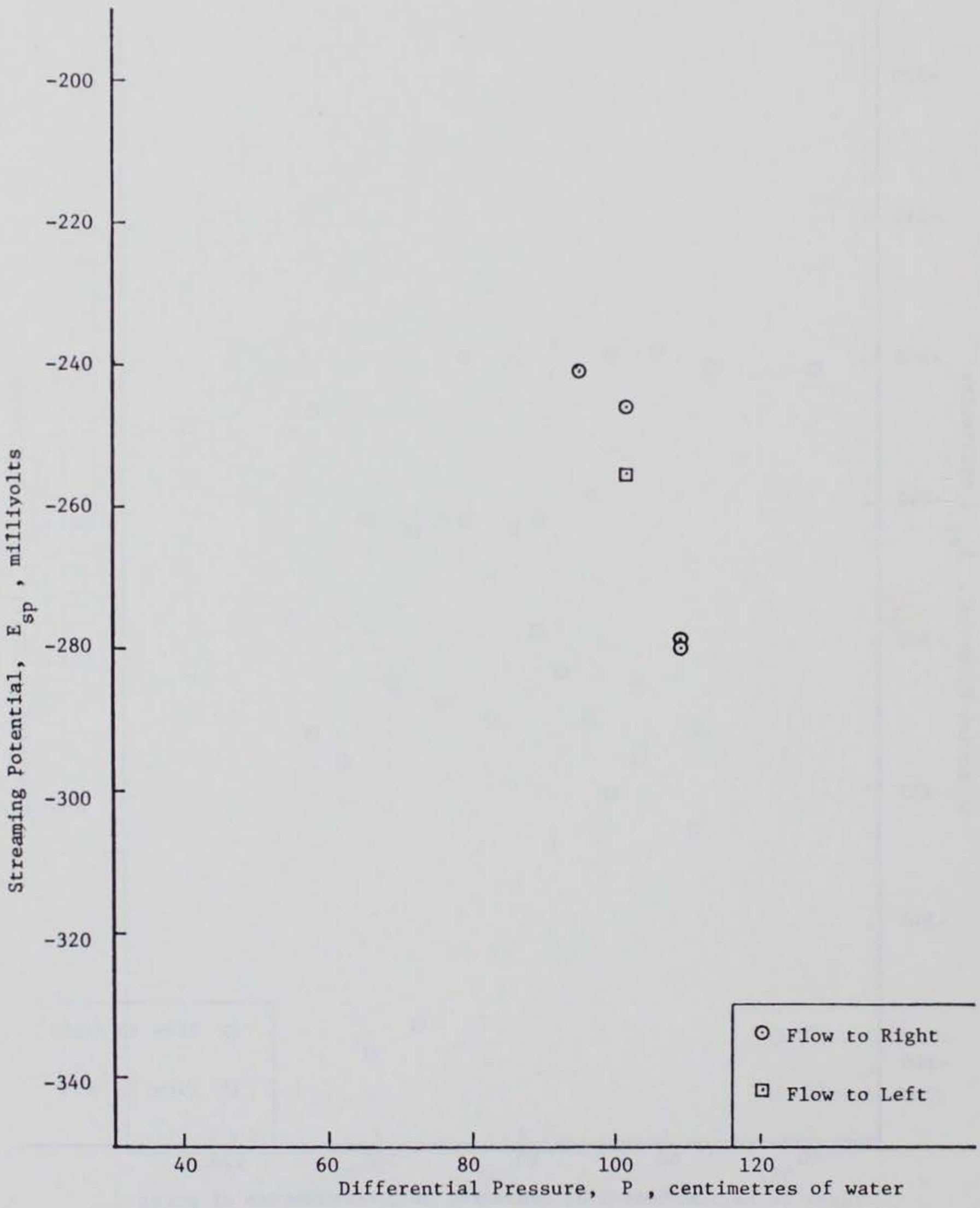

Figure 11. Streaming potential versus differential pressure, limestone gravel medium

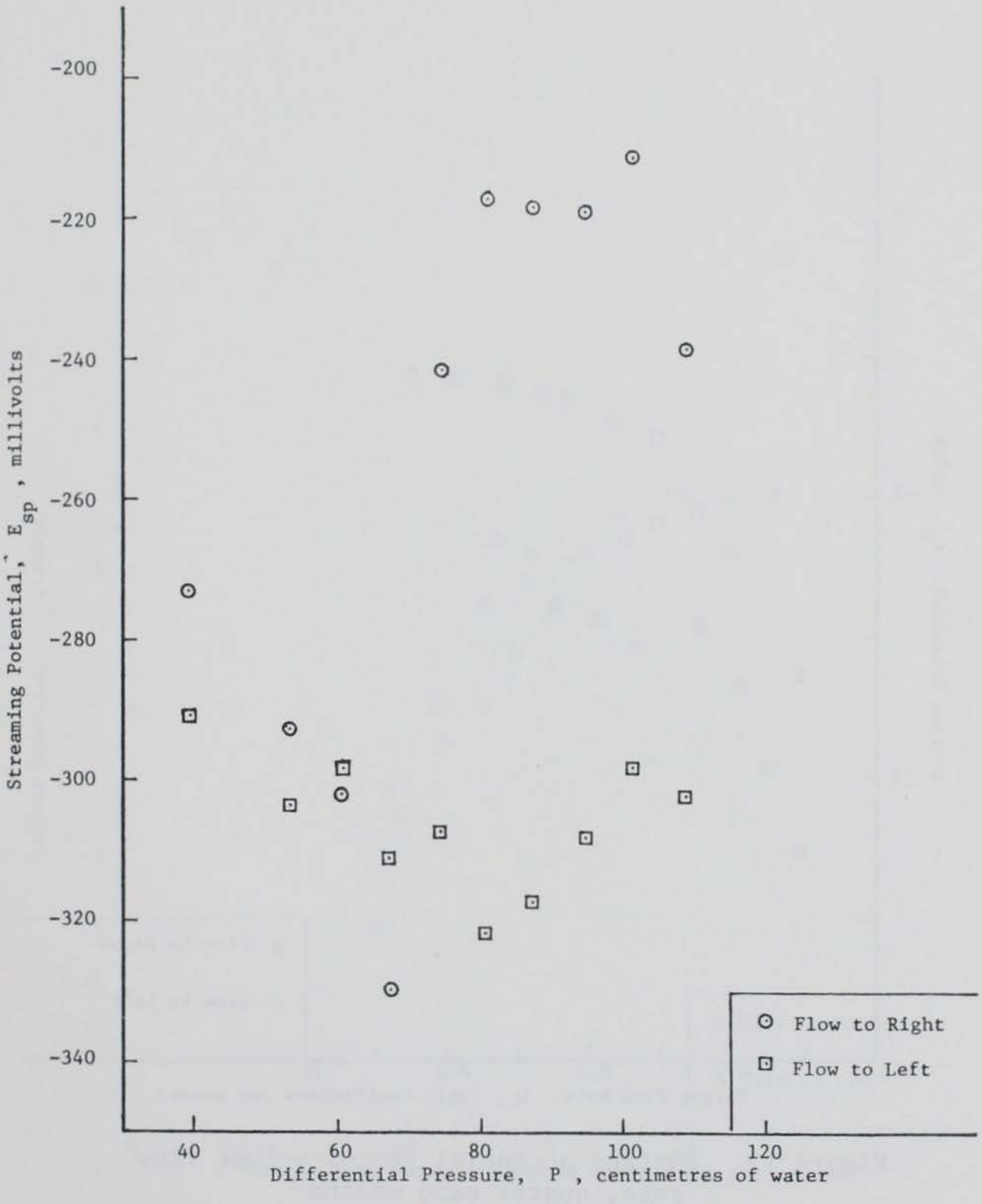

Figure 12. Streaming potential versus differential pressure, sand over soil media

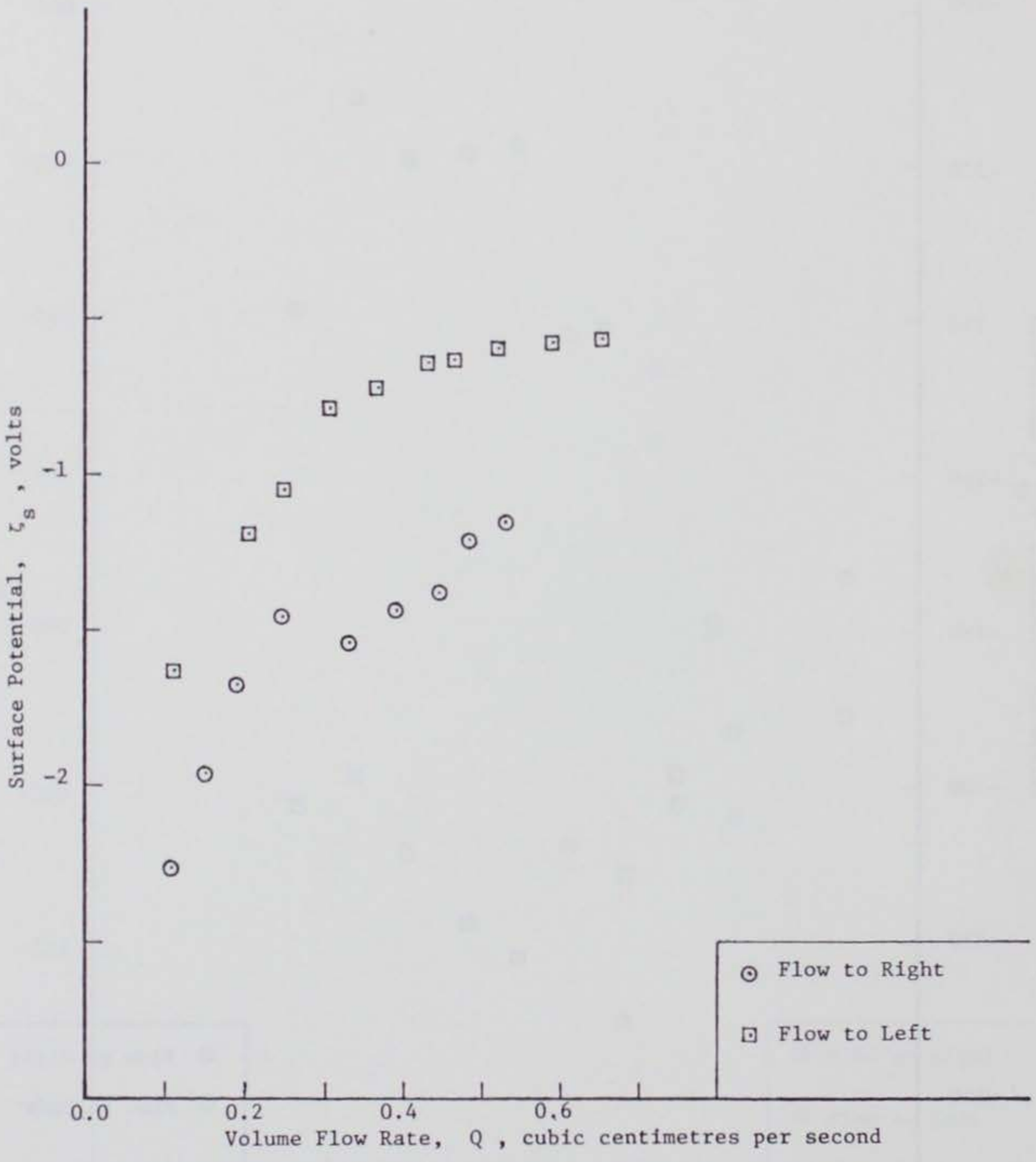

Figure 13. Surface potential versus volume flow rate, quartz sand medium

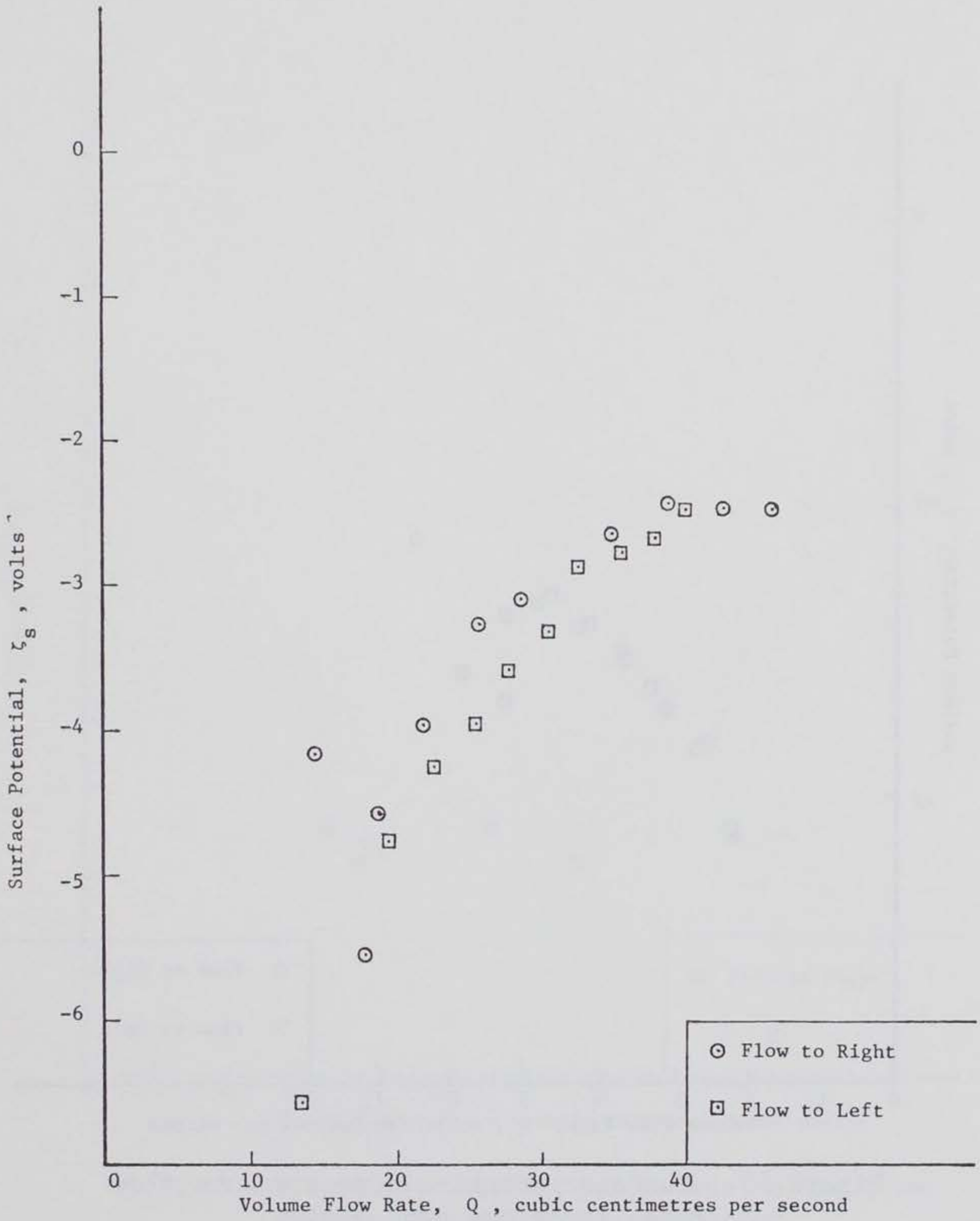

Figure 14. Surface potential versus volume flow rate, chert pea gravel medium

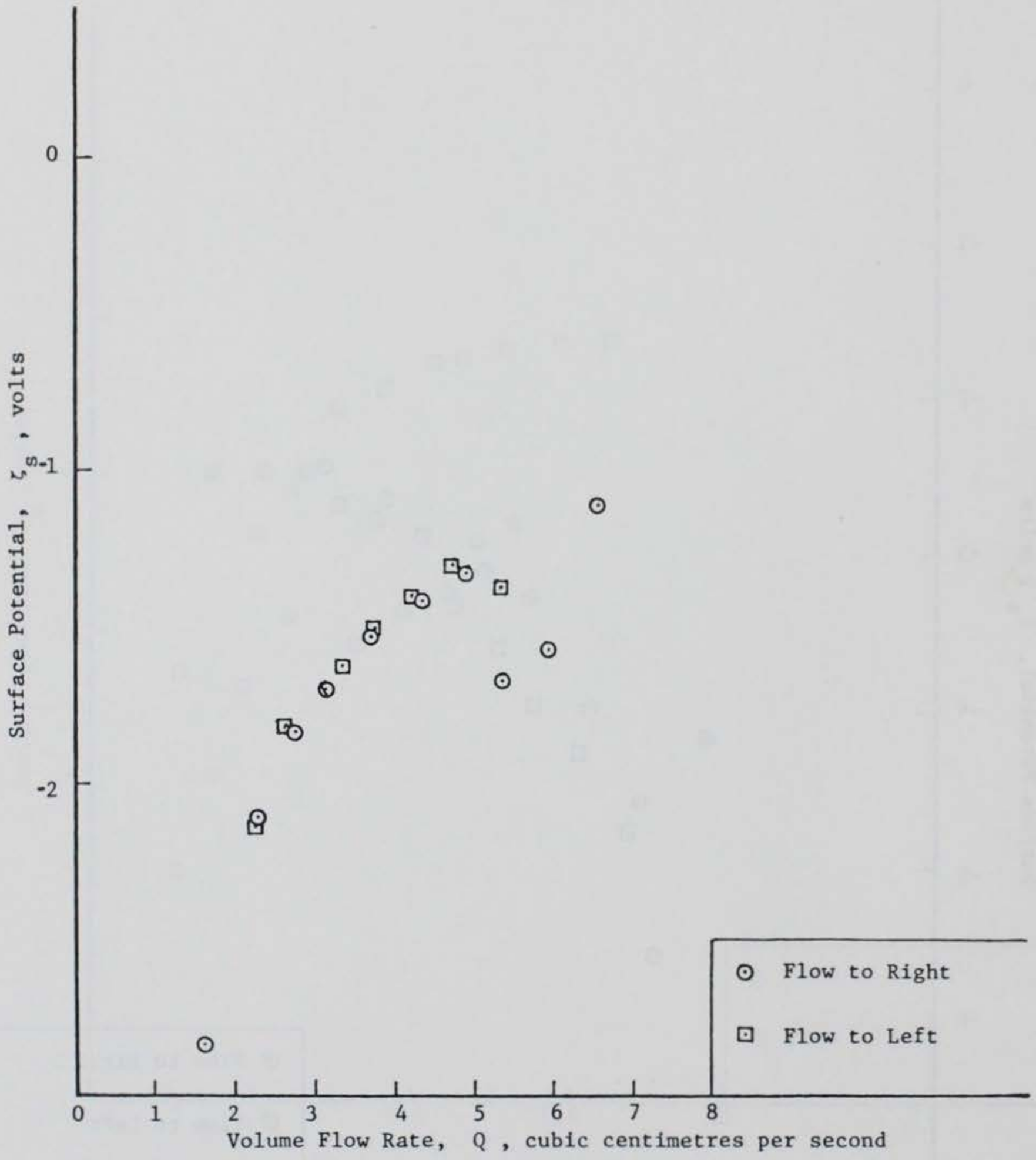

Figure 15. Surface potential versus volume flow rate, limestone sand medium

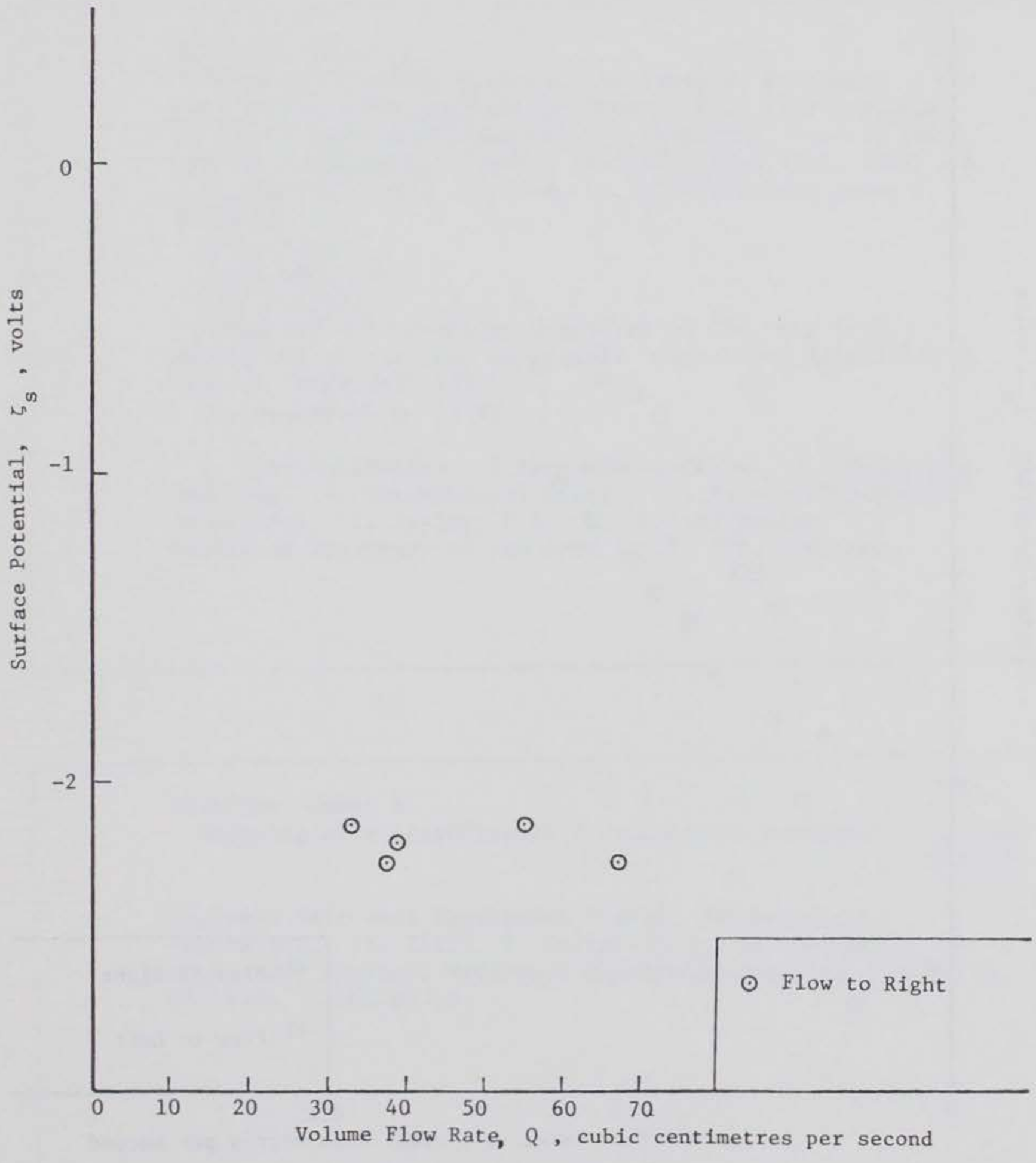

Figure 16. Surface potential versus volume flow rate, limestone gravel medium

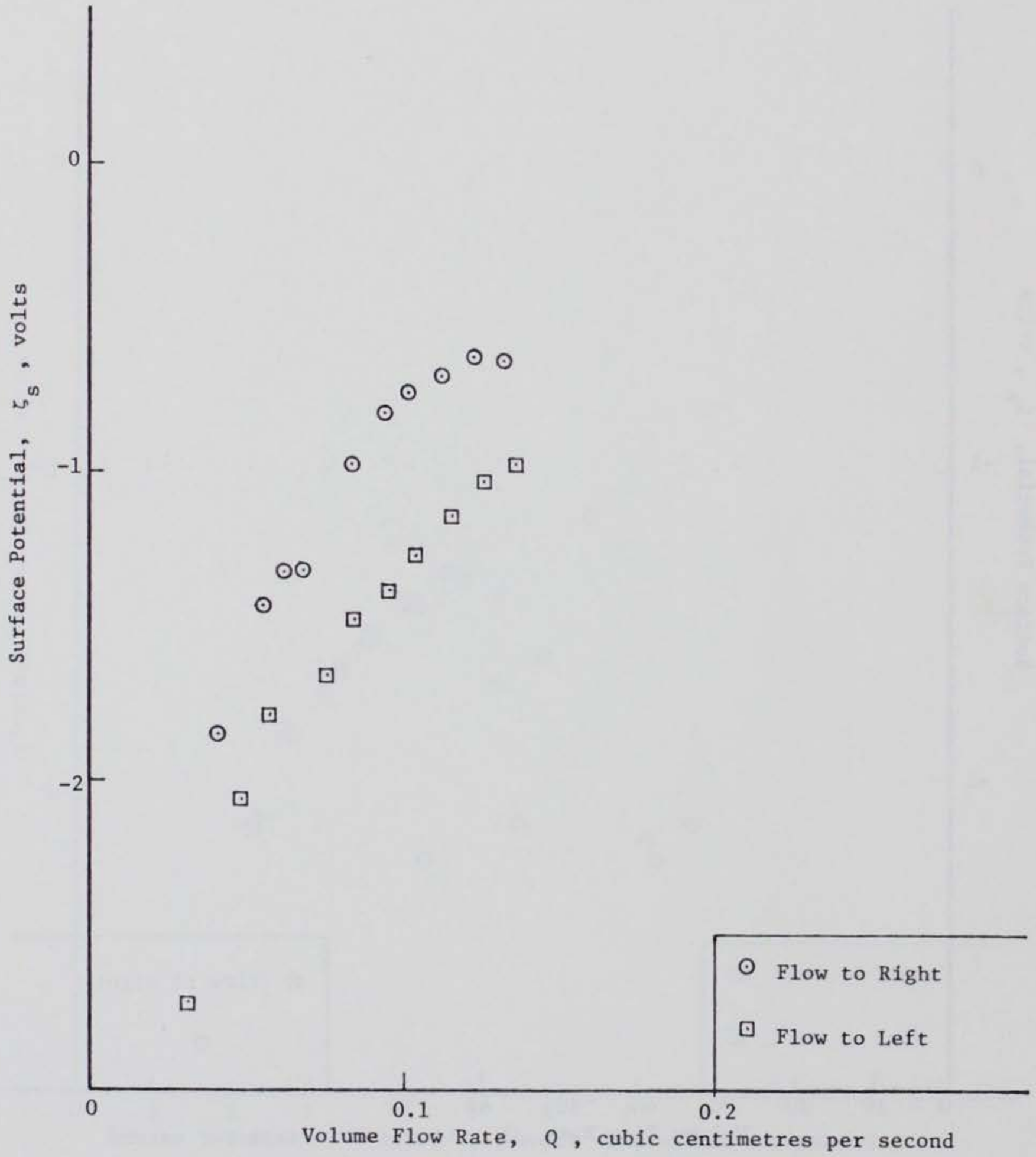

Figure 17. Surface potential versus volume flow rate, sand over soil media